Molecular Pharmacology Fast Forward. Published on February 12, 2016 as DOI: 10.1124/mol.115.101949
This article has not been copyedited and formatted. The final version may differ from this version.

Title page

Distinct phosphorylation clusters determine the signalling outcome of the free fatty acid receptor FFA4/GPR120

Rudi Prihandoko, Elisa Alvarez-Curto, Brian D. Hudson, Adrian J. Butcher, Trond Ulven, Ashley M. Miller, Andrew B. Tobin and Graeme Milligan

Medical Research Council Toxicology Unit, University of Leicester, Leicester LE1 9HN, United Kingdom (RP, AJB, ABT)

Molecular Pharmacology Group, Institute of Molecular, Cell and Systems Biology, University of Glasgow, Glasgow G12 8QQ, Scotland, United Kingdom (EA-C, BDH, GM)

Institute of Cardiovascular and Medical Sciences, College of Medical, Veterinary and Life Sciences, University of Glasgow, Glasgow G12 8QQ, Scotland, United Kingdom (AMM)

Department of Physics, Chemistry and Pharmacy, University of Southern Denmark, Campusvej 55, DK-5230 Odense M, Denmark (TU)

Molecular Pharmacology Fast Forward. Published on February 12, 2016 as DOI: 10.1124/mol.115.101949
This article has not been copyedited and formatted. The final version may differ from this version.

Running Title Page

Running title: *Phosphorylation profile of mFFA4 determines signalling*

* To whom correspondence should be addressed: Graeme Milligan, Molecular Pharmacology Group, Institute of Molecular, Cell and Systems Biology, College of Medical, Veterinary and Life Sciences, University of Glasgow, Glasgow G12 8QQ, Scotland, United Kingdom (Graeme.Milligan@glasgow.ac.uk) or Andrew B. Tobin, Medical Research Council Toxicology Unit, University of Leicester, Hodgkin building, Lancaster Road, Leicester LE1 9HN, United Kingdom (tba@leicester.ac.uk)

Manuscript information

Text Pages:

Tables: 2

Figures: 10

Words in Abstract: 249 words

Words in Introduction: 503 words

Words in Discussion: 1426 words

References: 51

Non-standard Abbreviations

αLA, α-linolenic acid; BRET, bioluminescence resonance energy transfer; CIAP, calf intestinal alkaline phosphatase; CHO, Chinese hamster ovary; DHA, docosahexaenoic acid; ECL,

Molecular Pharmacology Fast Forward. Published on February 12, 2016 as DOI: 10.1124/mol.115.101949
This article has not been copyedited and formatted. The final version may differ from this version.

enhanced chemiluminescence; eYFP, enhanced yellow fluorescent protein; GPCR, G protein-coupled receptor; Rluc, *Renilla* luciferase; TBST, Tris-buffered salt plus Tween 20

Molecular Pharmacology Fast Forward. Published on February 12, 2016 as DOI: 10.1124/mol.115.101949
This article has not been copyedited and formatted. The final version may differ from this version.

Abstract

It is established that long-chain free fatty acids including ω-3 fatty acids mediate an array of biological responses through members of the free fatty acid receptor family, which includes FFA4. However, the signalling mechanisms and modes of regulation of this receptor class remain unclear. Here we employ mass spectrometry to determine that phosphorylation of mouse (m)FFAR4 occurs at five serine and threonine residues clustered in two separable regions of the C terminal tail, designated cluster 1 (Thr^{347}, Thr^{349} and Ser^{350}) and cluster 2 (Ser^{357} and Ser^{361}). Mutation of these phospho-acceptor sites to alanine completely prevented phosphorylation of mFFA4 but did not limit receptor coupling to ERK1/2 activation. Rather an inhibitor of $G_q/_{11}$ proteins completely prevented receptor signalling to ERK1/2. In contrast, the recruitment of arrestin 3, receptor internalization and activation of Akt were regulated by mFFA4 phosphorylation. The analysis of mFFA4 phosphorylation-dependent signalling was extended further by selective mutations of the phospho-acceptor sites. Mutations within cluster 2 did not affect agonist activation of Akt but instead significantly compromised receptor internalization and arrestin 3 recruitment. Distinctly, mutation of the phospho-acceptor sites within cluster 1 had no effect on receptor internalization and a less extensive effect on arrestin 3 recruitment, but significantly uncoupled the receptor from Akt activation. These unique observations define differential effects on signalling mediated by phosphorylation at distinct locations. This hallmark feature supports the possibility that the signalling outcome of mFFA4 activation can be determined by the pattern of phosphorylation (phosphorylation barcode) at the C-terminus of the receptor.

Molecular Pharmacology Fast Forward. Published on February 12, 2016 as DOI: 10.1124/mol.115.101949
This article has not been copyedited and formatted. The final version may differ from this version.

Introduction

Rather than acting simply as sources of energy, in recent times fatty acids derived from the diet have been appreciated to also act as signalling molecules that play integrative roles in dietary homeostasis (Dranse et al., 2013; Hara et al., 2014; Offermanns, 2014). Key contributions of such fatty acids to metabolic and inflammatory control, and to dysregulation of processes that are associated with obesity and metabolic syndrome (Oh et al., 2014; Sekiguchi et al., 2015; Watterson et al., 2014), are produced via specific interactions with G protein-coupled receptors (GPCRs) present at the surface of cells within tissues, including the gut, pancreas and adipose tissue, that control metabolite distribution, flux and storage (Oh et al., 2014; Sekiguchi et al., 2015; Watterson et al., 2014). Two GPCRs, FFA1 (also known as GPR40) and FFA4 (also known as GPR120) are known to respond selectively to longer chain free fatty acids (Milligan et al., 2015). FFA1 is highly expressed by pancreatic β-cells (Mancini and Poitout, 2013) and plays a key role in stimulating release of insulin in a glucose-concentration-dependent manner (Mancini and Poitout, 2013). This receptor has attracted considerable attention as a means to control glucose homeostasis and, therefore, as a potential therapeutic target for the treatment of type II diabetes (Mancini and Poitout, 2013). Indeed, the FFA1 agonist fasiglifam entered phase III clinical trials but, although clearly able to regulate glycaemia and to produce clinically relevant lowering of HbA1c levels in type II diabetes patients (Kaku et al., 2015; Mancini and Poitout, 2013; Mancini and Poitout, 2015), it was withdrawn from further trials over concerns of possible liver toxicity. Whilst FFA4 is also expressed in the pancreas (Stone et al., 2014; Suckow et al., 2014), where it may play roles in the regulation of glucagon production (Suckow et al., 2014), it is also expressed in various enteroendocrine cells (Iwasaki et al., 2015; Liu et al., 2015; Parker et al., 2009), in adipocytes (Liu et al., 2015; Oh et al., 2010; Oh et al., 2014) and

macrophages (Im, 2015; Liu et al., 2015; Oh et al., 2010; Oh et al., 2014). Potential combinations of effects on the release of incretins and/or satiety-regulating hormones in the gut, differentiation of and uptake of glucose by adipocytes, and control of the release of inflammatory mediators by macrophages, has suggested that FFA4 might also be a useful therapeutic target to modulate insulin resistance and glucose homeostasis (Ichimura et al., 2014; Liu et al., 2015; Milligan et al., 2015; Oh et al., 2014). A non-synonymous polymorphic variant of FFA4 has been reported to be linked to obesity in man (Ichimura et al., 2012), however, this variant does not appear to be linked to risk of type II diabetes or variation of fasting insulin levels (Bonnefond et al., 2015). However, genetic elimination of FFA4 in mouse has been noted to result in obesity, glucose intolerance and fatty liver with decreased adipocyte differentiation when such animals are fed a high-fat diet (Ichimura et al., 2012).

Murine models of diabetes and obesity make important contributions to pre-clinical predictions and decisions regarding possible therapeutic approaches. Therefore, understanding details of the responsiveness, function and regulation of murine (m)FFA4 in response to both endogenously generated and synthetic ligands (Oh et al., 2014), and how these may vary compared to the human receptor is vital. Herein we address these issues by exploring both G protein-dependent and -independent signals produced by mFFA4, defining sites of regulatory phosphorylation on the receptor and by generating and employing phospho-site specific antibodies that can define the intrinsic activity state of the receptor *in situ*. In this way we describe here the signalling responses that are regulated by mFFA4 phosphorylation within two clusters of phospho-acceptor sites at the C-terminal tail of the receptor.

Molecular Pharmacology Fast Forward. Published on February 12, 2016 as DOI: 10.1124/mol.115.101949
This article has not been copyedited and formatted. The final version may differ from this version.

Materials and Methods

Materials

Unless otherwise stated, all biochemicals and reagents were from Sigma-Aldrich Co. (Dorset, UK). Tissue culture reagents and buffers were from Life Technologies Inc. (Paisley, UK). Primers were purchased from Thermo Fisher Scientific (Ulm, Germany). TUG-891 (3-(4-((4-fluoro-4′-methyl-[1,1′-biphenyl]-2-yl)methoxy)phenyl)-propanoic acid) was synthesized as described previously (Shimpukade et al., 2012). Compound 39 was synthesized according to Sparks et al., (Sparks et al., 2014). This compound is also known as AH 7614 and can be purchased from Tocris. The G_q/G_{11} inhibitor YM-254890 was a kind gift of Astrellas Pharma Inc. (Osaka, Japan). Cellular signalling assay kits (pAkt-Ser^{473}, pERK1/2) were obtained from Cisbio Bioassays (Codolet, France). Antibodies (pAkt-Ser^{473}, pERK1/2 and total ERK1/2) were obtained from Santa Cruz Biotechnology Inc (Heidelberg, Germany). Anti-GFP mouse monoclonal and anti-GFP rabbit polyclonal antibodies were purchased from Abcam (Cambridge, UK). Protease and phosphatase inhibitor cocktails were from Roche Applied Science (Burgess Hill, UK). [^{32}P]-orthophosphate (5 mCi, 185 MBq) was from PerkinElmer. Enhanced chemiluminescence (ECL) developing reagent was from Millipore (Watford, UK). Protein A sepharose beads, ECL and X-ray films were obtained from GE Healthcare (Amersham, Buckinghamshire, UK). Xograph compact x2 film developer and developing solutions were obtained from Xograph Healthcare (Gloucestershire, UK).

Plasmids and mutagenesis- To generate an HA epitope-tagged form of mFFA4, the receptor coding sequence was amplified by PCR that incorporated the HA tag sequence at the C-terminal end followed by a stop codon. The mFFA4 receptor was also fused at its C-terminus to enhanced yellow fluorescent protein (eYFP) and to an N-terminal FLAG epitope in

Molecular Pharmacology Fast Forward. Published on February 12, 2016 as DOI: 10.1124/mol.115.101949
This article has not been copyedited and formatted. The final version may differ from this version.

pcDNA5/FRT/TO. This construct was used as template to generate various mutants (see Results) using the Quickchange II method (Stratagene, UK). The identity of all new constructs generated was verified by nucleotide sequencing. Bovine arrestin 3 was fused to *Renilla* luciferase (Rluc) as previously described (Hudson et al., 2014; MacKenzie et al., 2014).

Cell lines- Flp-In^{TM} T-REx^{TM} 293 cells able to express constructs of interest from the tetracycline/doxycycline T-REx^{TM} -inducible locus were generated by co-transfecting FLAG-mFFA4-eYFP or one of the mutants (FLAG-mFFA4-TDTS-AAA-eYFP, FLAG-mFFA4-ADAA-SSS-eYFP or FLAG-mFFA4-ADAA-AAA-eYFP) with the pOG44 plasmid into parental Flp-In^{TM} T-REx^{TM} 293 cells (Life Technologies Inc, Paisley, UK). Following transfection, 200 μg.ml^{-1} of hygromycin B was added to the culture medium allowing for polyclonal selection of cells. Chinese hamster ovary (CHO) cells which stably and constitutively expressed the non C-terminally tagged, C-terminal HA or eYFP epitope-tagged mFFA4 or mFFA4 containing mutations within the C-terminal tail were generated using the Flp-In^{TM} system. CHO Flp-In^{TM} cells (Life Technologies Inc) were co-transfected with pcDNA5/FRT containing mFFA4 and pOG44, transfected cells were selected with 400 μg/ml hygromycin B and expression of mFFA4 was confirmed by immunoblotting with anti-HA or anti-GFP antibody.

[^{32}P]-Orthophosphate labelling and mFFA4 immunoprecipitation- CHO Flp-In^{TM} cells expressing mFFA4 were seeded at 200.000 cells/well in 6-well plates and grown for 48 h. They were then serum starved overnight at 37^{o}C. Cells were washed three times in 1 ml phosphate free Krebs/HEPES buffer (10 mM HEPES, 118 mM NaCl, 4.69 mM KCl, 1.18 mM $MgSO_4.7H_2O$, 1.3 mM $CaCl_2$, 25.0 mM $NaHCO_3$, 11.7 mM glucose, pH 7.4) and then incubated with 100 μCi/ml [^{32}P]-orthophosphate for 1.5 h at 37^{o}C. Cells were treated with ligands for an appropriate

Molecular Pharmacology Fast Forward. Published on February 12, 2016 as DOI: 10.1124/mol.115.101949
This article has not been copyedited and formatted. The final version may differ from this version.

time at 37°C. The reactions were terminated by rapid aspiration of the buffer followed by addition of 1 ml ice-cold radioimmunoprecipitation (RIPA) buffer (10 mM Tris, 2 mM EDTA, 20 mM glycerol-2-phosphate, 160 mM NaCl, 1% v/v Nonidet-P40, 0.5% w/v sodium deoxycholate, pH 7.4) for 30 min on ice. Cell lysates were cleared by centrifugation (20000 x g for 10 min) and receptors were immunoprecipitated from pre-cleared lysates using 1 µg/sample of the appropriate antibody for 1 h or overnight at 4°C. Immunocomplexes were isolated on protein A-sepharose beads and the beads were washed three times with ice-cold buffer (10 mM Tris, 2 mM EDTA, 20 mM glycerol-2-phosphate, pH 7.4). Immunocomplexes were resuspended in 2x SDS-PAGE sample buffer (125 mM Tris, 200 mM dithiothreitol, 4% SDS, 20% glycerol and 0.05% bromophenol blue, pH 6.8) and placed in a 60°C water bath for 3-5 min. Receptor proteins were resolved on 10% SDS-PAGE gels (200v, 1 h 20 min) and electroblotted onto nitrocellulose membranes using the semi-dry transfer method and Tris-Glycine transfer buffer (25 mM Tris, 190 mM Glycine, 20% methanol). Receptor phosphorylation was detected on X-ray films and developed using Xograph film developer. The films were scanned and bands were quantified using AlphaImager software (Alpha Innotech, San Leandro, CA). Parallel western blotting was performed on the immunoprecipitated samples to check for loading consistency.

mFFA4 purification and mass spectrometry- Cells were stimulated with 10 µM TUG-891 for 5 min at 37°C and then harvested using PBS/1 mM EDTA (pH 7.4). Membranes were prepared and receptors were solubilized in PBS/1% NP-40 supplemented with protease and phosphatase inhibitors for 4 h at 4°C. Samples were centrifuged (20000 x g, 20 min) and the receptors in the supernatant were immunoprecipitated using anti-HA antibody coupled to agarose beads. The purified receptors were resolved on 8% SDS-PAGE gel and the gel was stained with colloidal Coomassie blue to reveal receptor band(s). The bands were excised and cut into 1-2

Molecular Pharmacology Fast Forward. Published on February 12, 2016 as DOI: 10.1124/mol.115.101949
This article has not been copyedited and formatted. The final version may differ from this version.

mm squares and then incubated with 1 µg sequencing grade trypsin (Promega, Southampton, UK) in 50 mM ammonium bicarbonate overnight at 37^{o}C. The supernatant was transferred to fresh tubes and the gel pieces were washed twice with 0.1% trifluoroacetic acid dissolved in 50% acetonitrile. The supernatants were pooled and subjected to LC MS/MS analysis.

LC-MS/MS was carried out using an LTQ Orbitrap mass spectrometer (Thermofisher Scientific, Rockford, IL). The pooled supernatants containing receptor peptides were loaded at high flow rate onto a reverse-phase trapping column (0.3mm i.d. x 1mm), containing 5µm C18 300 Å Acclaim PepMap media (Dionex, UK) and eluted through a reverse-phase capillary column (75µm i.d. x 150mm) containing Symmetry C18 100 Å media (Waters, Elsetree, U.K.) that was self-packed using a high pressure packing device (Proxeon Biosystems, Odense, Denmark). The resulting spectra were searched against the UniProtKB/SwissProt database using MASCOT (Matrix Science Ltd.) software with peptide tolerance set to 5 ppm and the MS/MS tolerance set to 0.6 Da. Fixed modifications were set as carbamidomethyl cysteine with variable modifications of phospho-serine, phospho-threonine, phospho-tyrosine and oxidized methionine. The enzyme was set to Trypsin/P and up to 2 missed cleavages were allowed. Peptides with a Mascot score greater than 20 and where the probability P that the observed match was a random event was <0.05 were included in the analysis. The spectra of peptides reported as being phosphorylated were interrogated manually to confirm the precise sites of phosphorylation.

Generation of phosphorylation-site specific FFA4 antisera- Phosphorylation specific antisera were raised against two peptides; IFTDTS$_{(P)}$VRRNDLNDLS and GAIFT$_{(P)}$DTS$_{(P)}$VRRND, which correspond to amino acids 343–357 of mFFA4 in which Ser^{350} was phosphorylated in the first peptide and Thr^{347} and Ser^{350} were phosphorylated in the second peptide. The 87-day program, which included four immunizations, was performed by Eurogentec

Molecular Pharmacology Fast Forward. Published on February 12, 2016 as DOI: 10.1124/mol.115.101949
This article has not been copyedited and formatted. The final version may differ from this version.

(Leige Science Park, Seraing, Belgium). The resulting antiserum was purified against the immunizing peptide.

Antibody characterization using phosphatase treatment- To characterize potential phospho-specific antibodies, phosphatase treatment experiments were performed. Cells seeded at 200 000 cells/well in 6-well plates were grown for 48h at 37^{o}C and then serum starved overnight at 37^{o}C. Cells were stimulated with an agonist and the receptors were purified by immunoprecipitation as described above. The immunoprecipitated receptors were washed 3 x 150 µl with calf intestinal alkaline phosphatase (CIAP) buffer supplemented with protease inhibitors and 0.2% octyl glucoside. The beads were resuspended in 50 µl CIAP buffer in the presence of 40 U CIAP and incubated overnight at 37^{o}C. Positive controls which consist of immunoprecipitated receptors incubated in CIAP buffer were included. The CIAP buffer was aspirated and the beads were resuspended in SDS-PAGE sample buffer. Samples were run on 8% SDS-PAGE and analysed by western blotting.

Immunocytochemistry- CHO cells expressing FLAG-mFFA4-eYFP tagged receptors were seeded onto 20-mm glass coverslips for 48 h prior to experimentation. Cells were serum starved overnight at 37^{o}C and then treated with vehicle, the FFA4 antagonist compound 39 or agonist for the indicated time. Cells were fixed in PBS containing 4% paraformaldehyde for 30 min at room temperature. Phosphorylation specific antibody pThr^{347}/pSer^{350} was used at 0.52 ng/ml followed by Alexa Fluor^{TM} 546 goat anti-rabbit secondary antibody at 1:1000 dilution. Data were acquired using an LSM510 laser-scanning confocal microscope (Zeiss).

mFFA4-arrestin 3 interaction assay- Arrestin 3 recruitment to mFFA4 was assessed using a bioluminescence resonance energy transfer (BRET) assay (Butcher et al., 2014; Hudson et al., 2014; Jenkins et al., 2010; MacKenzie et al., 2014). Briefly, HEK293T cells were co-

Molecular Pharmacology Fast Forward. Published on February 12, 2016 as DOI: 10.1124/mol.115.101949
This article has not been copyedited and formatted. The final version may differ from this version.

transfected with arrestin 3-Rluc and eYFP-tagged receptor plasmids in a 1:4 ratio using polyethyleneimine. After 24 h incubation, cells were sub-cultured into poly-D-lysine coated white 96 well microplates and incubated for a further 24 h prior to the assay. Cells were washed and incubated in Hanks' Balanced Salts Solution for 30 min prior to conducting the assay. The luciferase substrate coelenterazine h (2.5 μM) (Nanolight Tech, Pinetop, CA) was added to the cells and incubated for 10 min at 37°C before test compounds were added. Following a further 5 min incubation at 37°C, luminescent emissions at 535 and 475 nm were measured using a PHERAstar *FS* (BMG Labtech, Aylesbury, UK). BRET signals were represented as the 535/475 ratio and for all mutant forms of mFFA4 the BRET ratios obtained were expressed as a percentage of the maximum ratio obtained for TUG-891 at the wild type receptor. Kinetic experiments of arrestin-3 recruitment were carried out on transiently transfected HEK293T cells by incubating the cells at 37°C in the PHERAstar FS after addition of 5 μM coelenterazine h, with BRET measurements taken at 6 s intervals. In these experiments, test compounds were added using PHERAstar FS injectors allowing for continuous measurement during and immediately following compound addition.

Visualization of mFFA4 Internalization- Flp-In™ T-REx™ 293 cells expressing the different mutant constructs were cultured on poly-D-lysine coated glass coverslips and cultured for 24 hours before treatment with doxycycline (100 ng.ml^{-1}) to induce receptor expression. Live cells were then imaged using a Zeiss VivaTome spinning disk confocal microscopy system (Karl Zeiss, Oberkochen, Germany). Images were taken before the addition of ligand, and every 5 minutes after ligand addition for a total of 60 minutes.

Cell Surface Enzyme-Linked Immunosorbent Assay (ELISA)- Flp-In™ T-REx™ 293 cells expressing the different constructs were cultured on poly-D-lysine coated flat bottom 96-well

Molecular Pharmacology Fast Forward. Published on February 12, 2016 as DOI: 10.1124/mol.115.101949
This article has not been copyedited and formatted. The final version may differ from this version.

plates for 24 hours before treatment with doxycycline (100 ng.ml^{-1}) and treated with ligand for the indicated times. Total receptor surface expression was measured on paraformaldehyde fixed cells. These were subsequently incubated in PBS containing 5% bovine serum albumin (BSA) to block nonspecific binding sites (30 minutes at room temperature), followed by incubation with an anti-FLAG monoclonal primary antibody (30 minutes at room temperature), and finally with an anti-mouse horseradish peroxidase conjugated secondary antibody (30 minutes at room temperature). Cells were washed 3 times with PBS before measuring Hoechst fluorescence using a PolarStar Omega plate reader (BMG Labtech, Offenburg, Germany). After washing a final time with PBS, and incubating with 3,3',5,5'-tetramethylbenzidine horseradish peroxidase substrate in the dark at room temperature, the absorbance at 620 nm was measured on a PolarStar Omega plate reader. To calculate surface expression, the 620 nm absorbance was corrected for cell number based on Hoechst fluorescence.

Akt(Ser473) phosphorylation assay- mFFA4 signalling to phospho-Akt Ser^{473} (also called protein kinase B) was detected by using the HTRF phospho-Akt (Ser^{473}) kit (Cisbio Biassays, Codolet, France). In brief, cells were seeded in 96 well plates at 20000 cells/well and grown for 48 hrs before being serum starved overnight at 37^{o}C. Cells were stimulated with an agonist for the indicated times and lysed with 50 µl of lysis buffer for 1 hr at RT. Lysates (16 µl) were transferred to 384 well plates and 4 µl of premixed d2/cryptate antibodies (1:1 v/v) were added to each lysate. The reaction mixtures were incubated for 2 hr at RT and the plate was read on the ClarioStar plate reader (BMG Labtech, Aylesbury, UK). For inhibition experiments, cells were treated with an inhibitor ($G\alpha_{q/11}$ inhibitor/pertussis toxin) for the indicated time before the addition of the agonist. Confirmatory assays were performed using western blotting with total

Molecular Pharmacology Fast Forward. Published on February 12, 2016 as DOI: 10.1124/mol.115.101949
This article has not been copyedited and formatted. The final version may differ from this version.

and phospho-Akt (Ser^{473}) antibody purchased from Santa Cruz Biotechnology Inc (Heidelberg, Germany).

ERK1/2 phosphorylation assay- Receptor-mediated ERK1/2 phosphorylation was determined by using the Cisbio HTRF phospho-ERK (Thr^{202}/Tyr^{204}) cellular assay kit in a protocol identical to the phospho-Akt assay above.

Immunoblotting- Nitrocellulose membranes containing resolved receptor proteins were incubated in blocking solution (20 mM Tris, 150 mM NaCl, 0.1% Tween-20 (TBST), 5% non-fat dried milk, pH 7.5) for 1 h at room temperature or overnight at 4^{o}C. Membranes were probed with the appropriate primary antibody (diluted in blocking solution) for 1 h at RT. Membranes were washed 3 x 15 min in TBST and then incubated with a secondary antibody (diluted in blocking solution) for 1 h at RT. Following 3 x 15 min washes in TBST the membranes were dried by blotting the edge onto a piece of tissue paper. The membranes were placed on glass plates and ECL developing reagent was added for 5 min. Immunoreactivity was captured on ECL films and developed using a Xograph film developer. The films were scanned and bands were quantified using AlphaImager software (Alpha Innotech, San Leandro, CA).

Data analysis- All data presented represent mean ± standard error of at least three independent experiments. Data analysis and curve fitting was carried out using the Graphpad Prism software package. Concentration-response data were fitted to three-parameter sigmoidal concentration-response curves. Statistical analyses were carried out using standard t-tests, 1-way analysis of variance with Tukey's post-hoc analysis, or 2-way analysis of variance combined with Bonferonni post-hoc analysis as appropriate.

Molecular Pharmacology Fast Forward. Published on February 12, 2016 as DOI: 10.1124/mol.115.101949
This article has not been copyedited and formatted. The final version may differ from this version.

Results

Murine FFA4 becomes phosphorylated in an agonist-dependent fashion- To investigate if the murine (m)FFA4 receptor becomes phosphorylated in an agonist-dependent manner we performed [^{32}P]-orthophosphate labelling of CHO Flp-In^{TM} cells stably expressing a form of mFFA4 that incorporated a C-terminal HA-epitope tag (mFFA4-HA). Subsequent to treatment of the cells with either vehicle, an ω-3 fatty acid agonist (α-linolenic acid (αLA, 100 μM)) or the synthetic FFA4 agonist TUG-891 (10 μM, **Figure 1**), samples were immunoprecipitated with anti-HA antibody, resolved by SDS-PAGE and exposed to X-ray film. Under basal conditions, [^{32}P] was incorporated predominantly into a polypeptide with molecular mass of ~45kDa (**Figure 1A**) which correlated with the molecular mass of the mFFA4 construct as determined in anti-HA immunoblots (**Figure 1B**). The extent of incorporation of the radiolabel was significantly increased in samples that had been exposed to either αLA or TUG-891 (**Figure 1C**). Global incorporation of [^{32}P] in response to treatment with TUG-891 was rapid, peaking within 3 minutes (**Figure 1D**). Although showing a tendency to decline, TUG-891-induced phosphorylation remained significantly elevated over vehicle treatment for at least 30 minutes (**Figures 1D-1F**). These data indicate that mFFA4 is phosphorylated in the basal state and undergoes a rapid and sustained increase in phosphorylation following agonist stimulation.

Agonist-mediated phosphorylation occurs within two clusters of residues within the intracellular C-terminal tail of mFFA4- To identify specific amino acids that became phosphorylated in response to TUG-891 we performed mass spectrometry. Phosphorylation of wild type mFFA4-HA was detected at multiple residues in these studies (**Figure 2**). We obtained excellent coverage of the intracellular domains of mFFA4 with identification of tryptic peptides containing more than 70% of the serine and threonine residues contained within the intracellular

Molecular Pharmacology Fast Forward. Published on February 12, 2016 as DOI: 10.1124/mol.115.101949
This article has not been copyedited and formatted. The final version may differ from this version.

loops and C-terminal tail. All the phosphorylation sites identified were within the C-terminal tail and appeared in two spatially resolved clusters. Cluster 1 contained phosphorylation sites on residues Thr^{347}, Thr^{349} and Ser^{350} and cluster 2 contained sites on Ser^{357} and Ser^{361}. Hence, five out of six serine/threonine residues in the C-terminal tail were phosphorylated. Despite identifying peptides containing the one remaining serine in this region there was no evidence from mass spectrometry that this residue, Ser^{360}, was phosphorylated.

Antisera generation and characterization- To further characterize the phosphorylation status of mFFA4 and its regulation we generated antisera predicted to specifically identify phosphorylation of both Thr^{347} and Ser^{350} of the receptor, or only of Ser^{350}. These residues were selected on the basis that phosphorylation at these amino acids was readily observed in the mass spectrometry studies and phospho-peptides containing these sites were predicted to be highly immunogenic. Following anti-GFP/eYFP immunoprecipitation of lysates from Flp-In™ CHO cells expressing a form of mFFA4 incorporating an N-terminal FLAG-epitope tag and C-terminal yellow fluorescent protein (eYFP) (FLAG-mFFA4-eYFP) and that that had been treated with TUG-891, immunoblotting with either $pThr^{347}$/$pSer^{350}$ or $pSer^{350}$ antibodies detected a ~80 kDa polypeptide that potentially reflected the appropriately phosphorylated form of the receptor (**Figures 3A, 3B**). Confirmation that the antibodies specifically identified phosphorylated forms of FLAG-mFFA4-eYFP was provided by pre-treatment of the samples with calf intestinal alkaline phosphatase (CIAP), to remove phosphate groups, prior to resolution by SDS-PAGE where neither pT^{347}/pS^{350} nor pS^{350} antisera were able to identify the FLAG-mFFA4-eYFP protein (**Figures 3A, 3B**). Immunoblots using an anti-GFP antiserum demonstrated the presence of similar levels of receptor protein in all samples (**Figure 3C**). Importantly, even without the immuno-enrichment provided by anti-GFP/eYFP immunoprecipitation the $pThr^{347}$/$pSer^{350}$ and

Molecular Pharmacology Fast Forward. Published on February 12, 2016 as DOI: 10.1124/mol.115.101949
This article has not been copyedited and formatted. The final version may differ from this version.

pSer^{350} antisera were both able to detect phosphorylated FLAG-mFFA4-eYFP in lysates of cells expressing the receptor construct and, as anticipated, recognition was enhanced substantially following treatment of the cells with TUG-891 (**Figures 3D-3F**).

Furthermore, the pThr347/pSer350 antibody was able to detect mFFA4 receptor phosphorylation in the presence and absence of C-terminal tail eYFP tag (**Supplementary Figure 1**). This suggests that at least for these two sites, the presence of eYFP tag at the C-terminal tail does not interfere with receptor phosphorylation.

Interestingly, although murine and human share a high degree of sequence similarity within the C-terminal tail, they are not identical. In particular, the epitope recognised by the antibodies in the mouse and human FFA4 receptors differ by two amino acid residues (mouse; GAIFTDTSVRRNDLS and human; GAILTDTSVKRNDLS). Neither the mFFA4 pThr^{347}/pSer^{350} nor mFFA4 pSer^{350} antibodies were able to identify human FLAG-FFA4-eYFP that had been phosphorylated by treatment with TUG-891 (**Figures 3D-3F**). The phospho-specific antibodies therefore displayed exquisite species selectivity, as previously also noted for equivalent phospho-specific antibodies to human FFA4 (Butcher et al., 2014). Phosphorylation of mFFA4 in response to TUG-891 as detected by the pThr^{347}/pSer^{350} antibodies was concentration-dependent (**Figure 4A**). Moreover, this effect of TUG-891 was blocked by co-addition of the FFA4 antagonist, compound 39 (Sparks et al., 2014) (**Figure 4B, 4D**) and this was also true for identification using the mFFA4 pSer^{350} antiserum (**Figure 4B**). As well as phosphorylation of mFFA4 by the synthetic agonist, activation of mFFA4 with either of the ω-3 fatty acids, α-linolenic acid (αLA) or docosahexaenoic acid (DHA) also resulted in phosphorylation of the receptor as detected by the pThr^{347}/pSer^{350} antiserum in a time-dependent and sustained fashion (**Figure 4C**).

Molecular Pharmacology Fast Forward. Published on February 12, 2016 as DOI: 10.1124/mol.115.101949
This article has not been copyedited and formatted. The final version may differ from this version.

The pThr^{347}/pSer^{350} antibodies were also capable of identifying TUG-891-activated mFFA4 in immunocytochemical studies. In Flp-In^{TM} CHO cells expressing FLAG-mFFA4-eYFP these antibodies illuminated the plasma membrane of agonist-treated cells and merging of images of the antibody staining with those of the location of the eYFP tag showed co-incidence (**Figure 5A**). pThr^{347}/pSer^{350} antibody staining was substantially less intense in vehicle-treated cells (**Figure 5B**) and cell surface staining was completely abolished in cells that had been pre-treated with the antagonist compound 39 (**Figure 5C**). These data, coupled with a lack of significant antibody staining of non-transfected cells (**Figure 5D**), indicated the specificity of the antibody recognition of the phosphorylated form(s) of the receptor (**Figure 5**).

Generation of phosphorylation-deficient mFFA4 variants- To define whether residues identified as being phosphorylated in the mass spectrometry studies played important roles in potential interactions between mFFA4 and arrestin 3, we generated a series of site-directed mutants of the receptor. [^{32}P]-orthophosphate labelling experiments were performed in Flp-In^{TM} CHO cells stably expressing either the wild type FLAG-mFFA4-eYFP construct or receptor variants that had been mutated to convert various serine and/or threonine residues to alanine (**Figure 6A**). Consistent with the data from mFFA4-HA **(Figure 1)**, the wild type construct, which due to the eYFP tag compared with the HA-tagged receptor in Figure 1 now migrated as a ~75kDa polypeptide, showed basal levels of phosphorylation in [^{32}P]-orthophosphate labelling experiments that significantly increased with agonist (TUG-891) stimulation (**Figure 6B**). The two clusters of serine/threonine phosphorylation sites identified by mass spectrometry (cluster 1: amino acids 347-350 and cluster 2: 357-361) were altered as either two separate groups or the two sets of mutations were combined to eliminate all the potential sites of phosphorylation (**Figure 6A**). The variant in which serine and threonine residues within cluster 1 (^{347}TDTS^{350})

Molecular Pharmacology Fast Forward. Published on February 12, 2016 as DOI: 10.1124/mol.115.101949
This article has not been copyedited and formatted. The final version may differ from this version.

were replaced with alanine (designated mFFA4-ADAA-SSS) was substantially less phosphorylated upon addition of TUG-891 (**Figure 6B**). Similarly, the variant (designated mFFA4-TDTS-AAA), in which the serine residues within cluster 2 (Ser^{357}, Ser^{360} and Ser^{361}) were replaced with alanine, also showed substantially lower incorporation of [^{32}P] following addition of TUG-891 (**Figure 6B**). Combination of these two groups of alterations produced a form of the receptor (mFFA4-ADAA-AAA) in which both basal and agonist-induced phosphorylation was absent (**Figure 6B**). This was despite this form of the receptor being expressed as well as wild type and the other two mutants (**Figure 6C**). The level of agonist-mediated phosphorylation of mFFA4-ADAA-SSS was similar to that of mFFA4-TDTS-AAA (**Figure 6D**), suggesting both clusters of Ser/Thr residues contribute to a similar extent to the phosphorylation capacity of mFFA4 in response to TUG-891. These phospho-acceptor variants also confirmed the specificity of the pT347/pS350 antiserum. Immunoblots performed on lysates from Flp-In™ T-REx™ 293 cells stably expressing eYFP tagged versions of each of the three mutants showed a lack of recognition of both mFFA4-ADAA-AAA and mFFA4-ADAA-SSS, either with or without treatment with TUG-891 (**Figure 6E**). In contrast, mFFFA4-TDTS-AAA was identified by the pT^{347}/pS^{350} antiserum in an agonist-dependent manner (**Figure 6E**). Identification of mFFFA4-TDTS-AAA was reduced, however, compared to the wild type receptor, despite maintaining the specific target epitope. This may reflect that the peptide antigen sequence contains other residues of mFFA4 that may help define quaternary structure of this region.

Interactions between mFFA4 and arrestin 3-Agonist-induced interactions between the mutant forms of mFFA4 and arrestin 3 (also sometimes designated β-arrestin 2) were then explored in a series of BRET studies performed in HEK293T cells co-expressing a form of

Molecular Pharmacology Fast Forward. Published on February 12, 2016 as DOI: 10.1124/mol.115.101949
This article has not been copyedited and formatted. The final version may differ from this version.

mFFA4-eYFP and arrestin 3 tagged with *Renilla* luciferase. In these studies stimulation of wild type FLAG-mFFA4-eYFP with TUG-891 produced a large, concentration-dependent (pEC_{50} = 7.00 +/- 0.07 mean +/- SEM, n = 22) increase in BRET signal (**Figure 7A**). Removal of all the phosphorylation sites contained in clusters 1 and 2 at the C-terminal tail of mFFA4 (mFFA4-ADAA-AAA) resulted in a substantial decrease in agonist-mediated interaction with arrestin 3 (**Figures 7A, B**). In these experiments the maximal BRET signal obtained with mFFA4-ADAA-AAA was only 19.7 +/- 1.2 % (n = 10) of that of wild type receptor (**Figures 7A, B**). Linked with the fact that mFFA4-ADAA-AAA showed no evidence of receptor phosphorylation (**Figure 6**), this supports the notion that agonist-induced recruitment of arrestin 3 to mFFA4 is largely dependent on receptor phosphorylation. We next tested the relative contributions of each of cluster 1 and cluster 2 phosphorylation sites to the recruitment of arrestin 3. Conversion of serine residues within cluster 2 to alanine (mFFA4-TDTS-AAA) had a significant impact on the interaction of arrestin 3, reducing the maximal BRET signal to 31.9 +/-2.3% (n = 7) of that observed for the wild type receptor (**Figure 7A, Table 1**). In the case of cluster 1 (mFFA4-ADAA-SSS), mutating the serine and threonine residues to alanine also resulted in a reduction in arrestin 3 recruitment (E_{max} 54.3 +/- 2.1 % (n = 12)) of that observed for the wild type receptor) but this was not to the same extent ($p < 0.001$) as that seen for the cluster 2 mutant (**Figure 7A, Table 1**). Equivalent conclusions as to the contribution of these two clusters to arrestin 3 recruitment were drawn from kinetic BRET experiments carried out by treating the cells with a single maximal concentration of TUG-891 (10 μM) and recording the receptor-arrestin 3 interaction over time (**Figure 7B**). Thus, it would appear that although cluster 1 and cluster 2 provide equal contribution to the overall phosphorylation of mFFA4 in response to agonist activation (**Figure 6**) cluster 2 has a larger impact on the recruitment of arrestin 3.

Molecular Pharmacology Fast Forward. Published on February 12, 2016 as DOI: 10.1124/mol.115.101949
This article has not been copyedited and formatted. The final version may differ from this version.

Relationship between receptor phosphorylation, arrestin 3 recruitment and mFFA4 internalization- Interactions with arrestins are frequently essential for agonist-induced receptor internalization (Luttrell and Gesty-Palmer, 2010; Marchese et al., 2008). To test the relationship between receptor phosphorylation, arrestin 3 recruitment and receptor internalization, both imaging of the cellular location of the eYFP tag (**Figure 8A**) and ELISA studies which measured removal of the N-terminal FLAG epitope tag from the surface of cells (**Figure 8B**) were used to define the extent of internalization of the FLAG-mFFA4-eYFP receptor constructs following exposure to TUG-891. Consistent with the canonical pathway, in which receptor phosphorylation promotes receptor-arrestin interaction, which in turn mediates receptor internalization, the variant mFFA4-ADAA-AAA, which contains alanines in place of all the serine/threonine residues in clusters 1 and 2 and interacted poorly with arrestin 3, showed a large reduction in TUG-891-mediated internalization (**Figures 8A, B**). Conversion to alanines of the cluster 2 phosphorylation sites (mFFA4-TDTS-AAA) also inhibited agonist-mediated internalization, and to the same extent as mutation of all the phospho-acceptor sites. In contrast, removal of cluster 1 phosphorylation sites (mFFA4-ADAA-SSS had no effect on TUG-891-induced receptor internalization (**Figures 8A, B**). Hence, as observed for arrestin 3 recruitment (**Figure 7**), phosphorylation of residues within cluster 2 have a larger impact on receptor internalization than phosphorylation within cluster 1.

Relationship between mFFA4 phosphorylation and coupling to ERK1/2 and protein kinase B/Akt- Agonist activation of FFA4 can result in downstream regulation of a number of signalling pathways. Although generally viewed as a receptor that couples selectively to G_q/G_{11} family G proteins (Butcher et al., 2014; Milligan et al., 2015), there are also reports of key functions of the receptor that reflect engagement with pertussis toxin-sensitive G_i-family proteins

Molecular Pharmacology Fast Forward. Published on February 12, 2016 as DOI: 10.1124/mol.115.101949
This article has not been copyedited and formatted. The final version may differ from this version.

(Engelstoft et al., 2013). In CHO cells stably expressing FLAG-mFFA4-eYFP addition of TUG-891 resulted in rapid phosphorylation of ERK1/2 MAP kinases. This effect was blocked completely by the selective $G_{q/}G_{11}$ inhibitor YM-254890 (Canals et al., 2006; Nishimura et al., 2010; Takasaki et al., 2004) (**Figure 9A**) indicating that mFFA4 coupling to ERK1/2 was transduced via $G_{q/}G_{11}$ proteins. In contrast, mFFA4 activation of protein kinase B/Akt was independent of $G_{q/}G_{11}$ proteins since this response was entirely unaffected by YM-254890 pre-treatment (**Figures 9B, C**). This was the case whether Akt phosphorylation was measured via an HTRF-based assay (**Figure 9B**) or in immunoblots using a pAkt Ser^{473} antibody (**Figure 9C**). We next assessed, therefore, whether TUG-891 produced phosphorylation of protein kinase B/Akt via a G_i-family G protein-mediated cascade. However, pre-treatment of cells with pertussis toxin to cause ADP-ribosylation of G_i-family G proteins also did not affect this pathway (**Figures 9D, 9E**) and again this was the outcome whether using HTRF- (**Figure 9D**) or immunoblot-based assays (**Figure 9E**).

It was possible that receptor phosphorylation-dependent pathways, rather than a canonical G protein-mediated pathway, might be responsible for coupling the mFFA4 to Akt signalling. The rapidly-induced peak of protein kinase B/Akt Ser^{473} phosphorylation was substantially lower for the combined cluster 1 and 2 mutant mFFA4-ADAA-AAA both in time-course experiments and in concentration-response studies employing TUG-891 (**Figures 10 A, B**) compared to wild type, indicating that receptor phosphorylation-dependent mechanisms do play a role in Akt signalling. Importantly, a similar reduction in peak AKT Ser^{473} phosphorylation was observed for the cluster 1 mutant, mFFA4-ADAA-SSS (**Figures 10A, B, Table 2**). Notably, by contrast, the peak Akt Ser^{473} phosphorylation response for the cluster 2 mutant mFFA4-TDTS-AAA was equivalent to that of the wild type receptor (**Figures 10A, B, Table 2**). Thus, mFFA4 phosphorylation appears

Molecular Pharmacology Fast Forward. Published on February 12, 2016 as DOI: 10.1124/mol.115.101949
This article has not been copyedited and formatted. The final version may differ from this version.

to play a role in coupling the receptor to Akt activation and that amino acids within cluster 1 (Thr^{347}, Thr^{349} and Ser^{350}) are the primary phosphorylation targets involved. By contrast, removal of serines and threonines in either cluster 1, cluster 2, or both groups did not uncouple mFFA4 signalling to ERK1/2 (**Figures 10C, D**). This demonstrates that receptor phosphorylation, arrestin 3 recruitment, and receptor internalization, all of which are disrupted in these mutants, have no role in coupling mFFA4 to the ERK1/2 pathway.

Discussion

Many GPCRs fashion cell type specific signals despite being activated by the same ligand(s). Although this is poorly explored, these differences may reflect the relative prevalence of distinct G protein-mediated and non-canonical pathways that a receptor can couple to in different cell types. Importantly, such variation expands the diversity and utility of endogenous ligands and their receptors (Thompson et al., 2014) beyond the currently fashionable view of 'biased' ligands that favor engagement with one signalling pathway over another in a single cell type (Luttrell et al., 2015; Violin et al., 2014). FFA4 is such a pleotropic GPCR (Milligan et al., 2015), able to generate a range of physiological endpoints in different cell types by engaging distinct signalling pathways. For example, although FFA4-mediates elevation of Ca^{2+} via G_q/G_{11} G proteins and hence promotes the release of incretin hormones, such as GLP-1, from enteroendocrine cells (Hirasawa et al., 2005), this receptor is also reported to regulate release of satiety promoting hormones from gut cells via activation of pertussis toxin-sensitive G_i-family G proteins (Engelstoft et al., 2013). Moreover, a number of anti-inflammatory effects of ω-3 fatty acids produced via macrophages are mediated by FFA4, reportedly via engagement with non-G

Molecular Pharmacology Fast Forward. Published on February 12, 2016 as DOI: 10.1124/mol.115.101949
This article has not been copyedited and formatted. The final version may differ from this version.

protein-dependent pathways involving recruitment of arrestin 3 and subsequent downstream interactions between TAB1 and TAK1 (Oh et al., 2010; Oh et al., 2014). Although there may be opportunities to identify agonist ligands at FFA4 that display marked bias in stabilizing conformations of the receptor that allow differential engagement with G_q/G_{11} versus G_i G-proteins or other pathways, current synthetic ligands of FFA4 are, in essence, carboxylic acid-containing, fatty acid like molecules (Milligan et al., 2015). Therefore, there is currently insufficient chemical diversity to hope to engage distinct signalling pathways with high selectivity compared to the endogenous ligands and to test this hypothesis directly.

In the absence of such ligands our approach has been to determine the sites of phosphorylation and, by mutating these sites, generate a mutant receptor that is not phosphorylated and is therefore uncoupled from phosphorylation-dependent processes such as receptor interaction with arrestins and receptor internalization. We have previously described these receptor mutants as G protein biased as they predominately coupled to heterotrimeric G proteins over non-canonical pathways such as those mediated by arrestins (Kong et al., 2010). Here we employed mass spectrometry to determine that mFFA4 shows agonist-regulated phosphorylation within two specific clusters of serine/threonine residues (cluster 1 and cluster 2) located within the C-terminal tail. Mutation of the observed phospho-acceptor amino acids to alanine resulted in a receptor that was fully resistant to agonist-induced phosphorylation. Interestingly, this receptor mutant coupled normally to the ERK1/2 pathway indicating that mFFA4 coupling to ERK1/2 was phosphorylation independent. Moreover, by employing an inhibitor of G_q/G_{11} proteins we were able to define that mFFA4 coupling to ERK was dependent on G protein signalling. This is in contrast to mFFA4 recruitment of arrestin 3, mFFA4 internalization and Akt activation which were all regulated by mFFA4 phosphorylation.

Molecular Pharmacology Fast Forward. Published on February 12, 2016 as DOI: 10.1124/mol.115.101949
This article has not been copyedited and formatted. The final version may differ from this version.

Thus, we were able to de-convolute the mFFA4 signalling responses that lay downstream of G protein coupling and mFFA4 phosphorylation.

One of the primary functions of GPCR phosphorylation is to promote the interaction of the receptor with members of the arrestin-adaptor protein family (arrestin 1-4) (Reiter and Lefkowitz, 2006). Although the extent to which phosphorylation increases the affinity of the activated receptor for an arrestin depends on the receptor subtype (see; (Tobin, 2008)) we show here that agonist-mediated recruitment of arrestin 3 to mFFA4 was almost totally dependent on phosphorylation of residues at the C-terminal tail of the receptor. In this respect mFFA4 behaves in a very similar manner to human FFA4 (Butcher et al., 2014). Also consistent with human FFA4, the phospho-acceptor sites on mFFA4 appeared in two clusters, cluster 1 (Thr^{347}, Thr^{349} and Ser^{350}) and cluster 2 (Ser^{357} and Ser^{361}). Based on incorporation of [^{32}P] orthophosphate each cluster contributed approximately equally to the overall phosphorylation of the receptor in response to agonist, however, phosphorylation at cluster 2 had a larger impact on arrestin 3recruitment. These data point towards site-specific roles for phosphorylation of mFFA4 and argues against the concept that phosphorylation at multiple sites at the C-terminal tail simply adds bulk negative charge which drives arrestin interaction, as has been suggested might be the case for rhodopsin (Ohguro et al., 1993).

Our study extended the analysis of the site-specific role of phosphorylation by consideration of other phosphorylation-dependent processes. This included receptor internalization that similarly was affected more by removal of the phosphorylation sites in cluster 2 than cluster 1. This correlates with reduced interaction with arrestin 3 seen in the cluster 2 mutant and is consistent with the known role of arrestins in driving receptor internalization (Shenoy and Lefkowitz, 2011). The relationship between receptor phosphorylation and the

Molecular Pharmacology Fast Forward. Published on February 12, 2016 as DOI: 10.1124/mol.115.101949
This article has not been copyedited and formatted. The final version may differ from this version.

activation of Akt was, however, more complex. Here the peak Akt response was significantly reduced by a mutant mFFA4 where all the phospho-acceptor sites were removed, indicating an important regulatory role of phosphorylation in this response. Selective removal of cluster 2 phospho-acceptor sites did not, however, significantly affect the Akt response. In contrast, removal of phospho-acceptor sites within cluster 1 had as large an effect on the Akt response as removal of all the phospho-acceptor sites in mFFA4. Therefore, these data further support the hypothesis that different sites of phosphorylation at the C-terminus of mFFA4 having different signalling outcomes.

As the cluster 1 mutant, despite showing poor interaction with arrestin 3, still activated Akt fully it might be concluded that arrestin 3 plays only a minor role in the activation of this pathway by mFFA4. However, neither blockade of G_q/G_{11} or G_i-G protein family interactions with the receptor affected this signal. Moreover, as a downstream measure of mFFA4 activation, it would be expected that regulation of Akt would show a significant degree of amplification and, therefore, substantially reduced interaction with arrestin 3 is compatible with maintenance of a level of signal generation. This is a common feature in 'knock-down' studies where a non-linear relationship between the degree of protein reduction and effect is often seen and is to be expected. Thus our data can be interpreted to indicate that phosphorylation at cluster 2 regulates Akt signalling in an arrestin-dependent manner. Moreover, a number of other receptors have also been shown to activate the Akt pathway in an arrestin-dependent manner (Cianfrocca et al., 2010; Kendall et al., 2014). Given the possibility that mFFA coupling to Akt is phosphorylation and arrestin 3 dependent it is possible that phosphorylation at either cluster 1 or 2 induces distinct and differential conformations of arrestin 3 and that these mediate different signalling outcomes from the arrestin. Assessing this hypothesis will be an important challenge for the

future. In the case of Akt activation, it may be that phosphorylation within cluster 2 induces an arrestin conformation that drives Akt activation. Removal of phospho-acceptor sites in cluster 2 will thereby prevent arrestin from adopting a conformation that mediates Akt signalling. We, and others, have suggested that the multi-site phosphorylation of GPCRs might represent a barcode that determines receptor-signalling outcomes and that by differential regulation of the phosphorylation barcode different signalling outcomes can be achieved (Butcher et al., 2011; Nobles et al., 2011; Tobin et al., 2008). It is possible that different phosphorylation barcodes mediate different arrestin conformations and that this results in different arrestin-dependent signalling (Nobles et al., 2011). Although it is now clear that arrestin adopts an active conformation on interaction with receptors (Zhuo et al., 2014) and that a recent crystal structure of arrestin in complex with a phosphorylated C-terminal tail peptide of a GPCR provides atomic level detail of the active arrestin conformation (Shukla et al., 2013) it is not yet clear whether differential phosphorylation can result in different active conformational states. Our data does, however, support the hypothesis that differential receptor phosphorylation can result in different signalling outcomes. In the case of mFFA4 it would appear that phosphorylation within cluster 1 can impact preferentially on arrestin interaction and receptor internalization whilst phosphorylation within cluster 2 has less impact on arrestin recruitment and internalization but, rather, preferentially regulates Akt signalling.

Our studies clearly predict that identification or design of novel mFFA4 ligands that drive differential phosphorylation at cluster 1 and cluster 2 would show differential coupling to phosphorylation-dependent processes that include arrestin recruitment, receptor internalization and Akt signalling. In this way an mFFA4 ligand that can modulate the site-specific phosphorylation of residues within cluster 1 and 2 would have a highly refined signalling profile

Molecular Pharmacology Fast Forward. Published on February 12, 2016 as DOI: 10.1124/mol.115.101949
This article has not been copyedited and formatted. The final version may differ from this version.

and, as a consequence, might activate a restricted number of physiological responses compared to a ligand that activated non-selectively both phosphorylation-dependent and independent signalling. This may be very important in the development of therapeutic compounds that target FFA4, for example to regulate glycaemia in type II diabetes (Milligan et al., 2015; Oh et al., 2014; Sekiguchi et al., 2015; Watterson et al., 2014), where it is desirable to activate those pathways that mediate therapeutically beneficial outcomes over pathways that lead to adverse/toxic responses. Thus, the study presented here might provide the framework to develop mFFA4 biased ligands that specifically promote signalling with improved therapeutic potential.

Acknowledgments

The authors would like to thank Dr John D. Pediani, University of Glasgow, for assistance with imaging experiments.

Authorship Contributions

Participated in research design: Milligan, Tobin, Ulven, Miller

Conducted experiments: Prihandoko, Alvarez-Curto, Butcher, Hudson

Contributed new reagents or analytic tools: Tobin, Ulven

Performed data analysis: Prihandoko, Alvarez-Curto, Butcher, Hudson

Wrote or contributed to writing of manuscript: Milligan, Tobin, Alvarez-Curto, Prihandoko

Molecular Pharmacology Fast Forward. Published on February 12, 2016 as DOI: 10.1124/mol.115.101949
This article has not been copyedited and formatted. The final version may differ from this version.

REFERENCES

Bonnefond A, Lamri A, Leloire A, Vaillant E, Roussel R, Levy-Marchal C, Weill J, Galan P, Hercberg S, Ragot S, Hadjadj S, Charpentier G, Balkau B, Marre M, Fumeron F and Froguel P (2015) Contribution of the low-frequency, loss-of-function p.R270H mutation in FFAR4 (GPR120) to increased fasting plasma glucose levels. *Journal of medical genetics* **52**(9): 595-598.

Butcher AJ, Hudson BD, Shimpukade B, Alvarez-Curto E, Prihandoko R, Ulven T, Milligan G and Tobin AB (2014) Concomitant action of structural elements and receptor phosphorylation determines arrestin-3 interaction with the free fatty acid receptor FFA4. *The Journal of biological chemistry* **289**(26): 18451-18465.

Butcher AJ, Prihandoko R, Kong KC, McWilliams P, Edwards JM, Bottrill A, Mistry S and Tobin AB (2011) Differential G-protein-coupled receptor phosphorylation provides evidence for a signaling bar code. *The Journal of biological chemistry* **286**(13): 11506-11518.

Canals M, Jenkins L, Kellett E and Milligan G (2006) Up-regulation of the angiotensin II type 1 receptor by the MAS proto-oncogene is due to constitutive activation of Gq/G11 by MAS. *The Journal of biological chemistry* **281**(24): 16757-16767.

Cianfrocca R, Rosano L, Spinella F, Di Castro V, Natali PG and Bagnato A (2010) Beta-arrestin-1 mediates the endothelin-1-induced activation of Akt and integrin-linked kinase. *Canadian journal of physiology and pharmacology* **88**(8): 796-801.

Dranse HJ, Kelly ME and Hudson BD (2013) Drugs or diet?--Developing novel therapeutic strategies targeting the free fatty acid family of GPCRs. *British journal of pharmacology* **170**(4): 696-711.

Engelstoft MS, Park WM, Sakata I, Kristensen LV, Husted AS, Osborne-Lawrence S, Piper PK, Walker AK, Pedersen MH, Nohr MK, Pan J, Sinz CJ, Carrington PE, Akiyama TE, Jones RM, Tang C, Ahmed K, Offermanns S, Egerod KL, Zigman JM and Schwartz TW (2013) Seven transmembrane G protein-coupled receptor repertoire of gastric ghrelin cells. *Molecular metabolism* **2**(4): 376-392.

Hara T, Kashihara D, Ichimura A, Kimura I, Tsujimoto G and Hirasawa A (2014) Role of free fatty acid receptors in the regulation of energy metabolism. *Biochimica et biophysica acta* **1841**(9): 1292-1300.

Hirasawa A, Tsumaya K, Awaji T, Katsuma S, Adachi T, Yamada M, Sugimoto Y, Miyazaki S and Tsujimoto G (2005) Free fatty acids regulate gut incretin glucagon-like peptide-1 secretion through GPR120. *Nature medicine* **11**(1): 90-94.

Hudson BD, Shimpukade B, Milligan G and Ulven T (2014) The molecular basis of ligand interaction at free fatty acid receptor 4 (FFA4/GPR120). *The Journal of biological chemistry* **289**(29): 20345-20358.

Ichimura A, Hasegawa S, Kasubuchi M and Kimura I (2014) Free fatty acid receptors as therapeutic targets for the treatment of diabetes. *Frontiers in pharmacology* **5**: 236.

Ichimura A, Hirasawa A, Poulain-Godefroy O, Bonnefond A, Hara T, Yengo L, Kimura I, Leloire A, Liu N, Iida K, Choquet H, Besnard P, Lecoeur C, Vivequin S, Ayukawa K,

Takeuchi M, Ozawa K, Tauber M, Maffeis C, Morandi A, Buzzetti R, Elliott P, Pouta A, Jarvelin MR, Korner A, Kiess W, Pigeyre M, Caiazzo R, Van Hul W, Van Gaal L, Horber F, Balkau B, Levy-Marchal C, Rouskas K, Kouvatsi A, Hebebrand J, Hinney A, Scherag A, Pattou F, Meyre D, Koshimizu TA, Wolowczuk I, Tsujimoto G and Froguel P (2012) Dysfunction of lipid sensor GPR120 leads to obesity in both mouse and human. *Nature* **483**(7389): 350-354.

Im DS (2015) Functions of omega-3 fatty acids and FFA4 (GPR120) in macrophages. *European journal of pharmacology*.

Iwasaki K, Harada N, Sasaki K, Yamane S, Iida K, Suzuki K, Hamasaki A, Nasteska D, Shibue K, Joo E, Harada T, Hashimoto T, Asakawa Y, Hirasawa A and Inagaki N (2015) Free fatty acid receptor GPR120 is highly expressed in enteroendocrine K cells of the upper small intestine and has a critical role in GIP secretion after fat ingestion. *Endocrinology* **156**(3): 837-846.

Jenkins L, Brea J, Smith NJ, Hudson BD, Reilly G, Bryant NJ, Castro M, Loza MI and Milligan G (2010) Identification of novel species-selective agonists of the G-protein-coupled receptor GPR35 that promote recruitment of beta-arrestin-2 and activate Galpha13. *The Biochemical journal* **432**(3): 451-459.

Kaku K, Enya K, Nakaya R, Ohira T and Matsuno R (2015) Efficacy and safety of fasiglifam (TAK-875), a G protein-coupled receptor 40 agonist, in Japanese patients with type 2 diabetes inadequately controlled by diet and exercise: a randomized, double-blind, placebo-controlled, phase III trial. *Diabetes, obesity & metabolism* **17**(7): 675-681.

Kendall RT, Lee MH, Pleasant DL, Robinson K, Kuppuswamy D, McDermott PJ and Luttrell LM (2014) Arrestin-dependent angiotensin AT1 receptor signaling regulates Akt and mTor-mediated protein synthesis. *The Journal of biological chemistry* **289**(38): 26155-26166.

Kong KC, Butcher AJ, McWilliams P, Jones D, Wess J, Hamdan FF, Werry T, Rosethorne EM, Charlton SJ, Munson SE, Cragg HA, Smart AD and Tobin AB (2010) M3-muscarinic receptor promotes insulin release via receptor phosphorylation/arrestin-dependent activation of protein kinase D1. *Proceedings of the National Academy of Sciences of the United States of America* **107**(49): 21181-21186.

Liu HD, Wang WB, Xu ZG, Liu CH, He DF, Du LP, Li MY, Yu X and Sun JP (2015) FFA4 receptor (GPR120): A hot target for the development of anti-diabetic therapies. *European journal of pharmacology*.

Luttrell LM and Gesty-Palmer D (2010) Beyond desensitization: physiological relevance of arrestin-dependent signaling. *Pharmacological reviews* **62**(2): 305-330.

Luttrell LM, Maudsley S and Bohn LM (2015) Fulfilling the Promise of "Biased" G Protein-Coupled Receptor Agonism. *Molecular pharmacology* **88**(3): 579-588.

MacKenzie AE, Caltabiano G, Kent TC, Jenkins L, McCallum JE, Hudson BD, Nicklin SA, Fawcett L, Markwick R, Charlton SJ and Milligan G (2014) The antiallergic mast cell stabilizers lodoxamide and bufrolin as the first high and equipotent agonists of human and rat GPR35. *Molecular pharmacology* **85**(1): 91-104.

Mancini AD and Poitout V (2013) The fatty acid receptor FFA1/GPR40 a decade later: how much do we know? *Trends in endocrinology and metabolism: TEM* **24**(8): 398-407.

Mancini AD and Poitout V (2015) GPR40 agonists for the treatment of type 2 diabetes: life after 'TAKing' a hit. *Diabetes, obesity & metabolism* **17**(7): 622-629.

Marchese A, Paing MM, Temple BR and Trejo J (2008) G protein-coupled receptor sorting to endosomes and lysosomes. *Annual review of pharmacology and toxicology* **48**: 601-629.

Milligan G, Alvarez-Curto E, Watterson KR, Ulven T and Hudson BD (2015) Characterizing pharmacological ligands to study the long-chain fatty acid receptors GPR40/FFA1 and GPR120/FFA4. *British journal of pharmacology* **172**(13): 3254-3265.

Nishimura A, Kitano K, Takasaki J, Taniguchi M, Mizuno N, Tago K, Hakoshima T and Itoh H (2010) Structural basis for the specific inhibition of heterotrimeric Gq protein by a small molecule. *Proceedings of the National Academy of Sciences of the United States of America* **107**(31): 13666-13671.

Nobles KN, Xiao K, Ahn S, Shukla AK, Lam CM, Rajagopal S, Strachan RT, Huang TY, Bressler EA, Hara MR, Shenoy SK, Gygi SP and Lefkowitz RJ (2011) Distinct phosphorylation sites on the beta(2)-adrenergic receptor establish a barcode that encodes differential functions of beta-arrestin. *Science signaling* **4**(185): ra51.

Offermanns S (2014) Free fatty acid (FFA) and hydroxy carboxylic acid (HCA) receptors. *Annual review of pharmacology and toxicology* **54**: 407-434.

Oh DY, Talukdar S, Bae EJ, Imamura T, Morinaga H, Fan W, Li P, Lu WJ, Watkins SM and Olefsky JM (2010) GPR120 is an omega-3 fatty acid receptor mediating potent anti-inflammatory and insulin-sensitizing effects. *Cell* **142**(5): 687-698.

Oh DY, Walenta E, Akiyama TE, Lagakos WS, Lackey D, Pessentheiner AR, Sasik R, Hah N, Chi TJ, Cox JM, Powels MA, Di Salvo J, Sinz C, Watkins SM, Armando AM, Chung H, Evans RM, Quehenberger O, McNelis J, Bogner-Strauss JG and Olefsky JM (2014) A Gpr120-selective agonist improves insulin resistance and chronic inflammation in obese mice. *Nature medicine* **20**(8): 942-947.

Ohguro H, Palczewski K, Ericsson LH, Walsh KA and Johnson RS (1993) Sequential phosphorylation of rhodopsin at multiple sites. *Biochemistry* **32**(21): 5718-5724.

Parker HE, Habib AM, Rogers GJ, Gribble FM and Reimann F (2009) Nutrient-dependent secretion of glucose-dependent insulinotropic polypeptide from primary murine K cells. *Diabetologia* **52**(2): 289-298.

Reiter E and Lefkowitz RJ (2006) GRKs and beta-arrestins: roles in receptor silencing, trafficking and signaling. *Trends in endocrinology and metabolism: TEM* **17**(4): 159-165.

Sekiguchi H, Kasubuchi M, Hasegawa S, Pelisch N, Kimura I and Ichimura A (2015) A novel antidiabetic therapy: free fatty acid receptors as potential drug target. *Current diabetes reviews* **11**(2): 107-115.

Shenoy SK and Lefkowitz RJ (2011) beta-Arrestin-mediated receptor trafficking and signal transduction. *Trends in pharmacological sciences* **32**(9): 521-533.

Shimpukade B, Hudson BD, Hovgaard CK, Milligan G and Ulven T (2012) Discovery of a potent and selective GPR120 agonist. *Journal of medicinal chemistry* **55**(9): 4511-4515.

Shukla AK, Manglik A, Kruse AC, Xiao K, Reis RI, Tseng WC, Staus DP, Hilger D, Uysal S, Huang LY, Paduch M, Tripathi-Shukla P, Koide A, Koide S, Weis WI, Kossiakoff AA, Kobilka BK and Lefkowitz RJ (2013) Structure of active beta-arrestin-1 bound to a G-protein-coupled receptor phosphopeptide. *Nature* **497**(7447): 137-141.

Sparks SM, Chen G, Collins JL, Danger D, Dock ST, Jayawickreme C, Jenkinson S, Laudeman C, Leesnitzer MA, Liang X, Maloney P, McCoy DC, Moncol D, Rash V, Rimele T, Vulimiri P, Way JM and Ross S (2014) Identification of diarylsulfonamides as agonists of the free fatty acid receptor 4 (FFA4/GPR120). *Bioorganic & medicinal chemistry letters* **24**(14): 3100-3103.

Stone VM, Dhayal S, Brocklehurst KJ, Lenaghan C, Sorhede Winzell M, Hammar M, Xu X, Smith DM and Morgan NG (2014) GPR120 (FFAR4) is preferentially expressed in pancreatic delta cells and regulates somatostatin secretion from murine islets of Langerhans. *Diabetologia* **57**(6): 1182-1191.

Suckow AT, Polidori D, Yan W, Chon S, Ma JY, Leonard J and Briscoe CP (2014) Alteration of the glucagon axis in GPR120 (FFAR4) knockout mice: a role for GPR120 in glucagon secretion. *The Journal of biological chemistry* **289**(22): 15751-15763.

Takasaki J, Saito T, Taniguchi M, Kawasaki T, Moritani Y, Hayashi K and Kobori M (2004) A novel Galphaq/11-selective inhibitor. *The Journal of biological chemistry* **279**(46): 47438-47445.

Thompson GL, Canals M and Poole DP (2014) Biological redundancy of endogenous GPCR ligands in the gut and the potential for endogenous functional selectivity. *Frontiers in pharmacology* **5**: 262.

Tobin AB (2008) G-protein-coupled receptor phosphorylation: where, when and by whom. *British journal of pharmacology* **153 Suppl 1**: S167-176.

Tobin AB, Butcher AJ and Kong KC (2008) Location, location, location...site-specific GPCR phosphorylation offers a mechanism for cell-type-specific signalling. *Trends in pharmacological sciences* **29**(8): 413-420.

Violin JD, Crombie AL, Soergel DG and Lark MW (2014) Biased ligands at G-protein-coupled receptors: promise and progress. *Trends in pharmacological sciences* **35**(7): 308-316.

Watterson KR, Hudson BD, Ulven T and Milligan G (2014) Treatment of type 2 diabetes by free Fatty Acid receptor agonists. *Frontiers in endocrinology* **5**: 137.

Zhuo Y, Vishnivetskiy SA, Zhan X, Gurevich VV and Klug CS (2014) Identification of receptor binding-induced conformational changes in non-visual arrestins. *The Journal of biological chemistry* **289**(30): 20991-21002.

Molecular Pharmacology Fast Forward. Published on February 12, 2016 as DOI: 10.1124/mol.115.101949
This article has not been copyedited and formatted. The final version may differ from this version.

FOOTNOTES

RP and EAC contributed equally to this work.

This work was supported by the following grants:

Biotechnology and Biosciences Research Council [BB/K019864/1]

Biotechnology and Biosciences Research Council [BB/K019856/1]

Medical Research Council Toxicology Unit [Core funding].

Molecular Pharmacology Fast Forward. Published on February 12, 2016 as DOI: 10.1124/mol.115.101949
This article has not been copyedited and formatted. The final version may differ from this version.

FIGURE LEGENDS

Figure 1: Murine FFA4 becomes phosphorylated in an agonist-dependent and sustained manner

Flp-In™ CHO cells stably expressing mFFA4-HA were labelled with [^{32}P]-orthophosphate and treated for 5 minutes (**A-C**) or for varying times (**D-F**) with vehicle (-) or the indicated concentrations of α-linolenic acid (αLA) or TUG-891. Following anti-HA immunoprecipitation samples were resolved by SDS-PAGE and subjected to autoradiography (**A, D**). Such autoradiograms were quantified by densitometry (**C, F**). Structure of TUG-891 is shown (**G**). Data are means +/- SEM. Significantly greater than vehicle treated **p < 0.01, *** p < 0.001. Similar levels of the receptor construct in each sample was demonstrated in anti-HA immunoblots (**B, E**). WB = western blot, Mono = monoclonal.

Figure 2: Mass spectrometry analysis of sites of agonist-promoted phosphorylation in mFFA4

CHO Flp-In™ cells stably expressing C-terminally HA-tagged mFFA4 and treated with TUG-891 (10 μM, 5 min) were used to immunoprecipitate and then digest the receptor for analysis using mass spectrometry. **A-E** representative mass spectra and associated fragmentation tables are shown that cover the five phosphorylated residues, Thr^{347}, Thr^{349}, Ser^{350} Ser^{357}, Ser^{361}, identified in various experiments. **F** shows a cartoon of mFFA4 with the sequence from the conserved NPXXY motif (NPILY in this receptor) at the bottom of transmembrane domain VII to the C-terminal tail, with amino acids denoted by the 'one letter' code. Amino acids that were identified as being phosphorylated are in **bold**. **G** provides a summary of the overall data set.

Molecular Pharmacology Fast Forward. Published on February 12, 2016 as DOI: 10.1124/mol.115.101949
This article has not been copyedited and formatted. The final version may differ from this version.

Figure 3: Generation and characterization of phospho-state specific mFFA4 antibodies

Antisera were generated against peptides incorporating either only phospho-Ser^{350} (**A, D**) or both phospho-Thr^{347} and phospho-Ser^{350} (**B, E**). Affinity purified antibodies were used to assess the phosphorylation status of FLAG-mFFA4-eYFP following treatment with vehicle or TUG-891 (10 μM, 5 min). Parallel immunoblots with an anti-GFP antiserum defined equal loading and levels of receptor expression in each sample (**C, F**). Confirmation that the phospho-Thr^{347}/Ser^{350} and phospho-Ser^{350} antibodies were indeed phospho site-specific was produced by pre-treating samples prior to resolution on SDS-PAGE with calf intestinal alkaline phosphatase (CIAP) (**A, B**). The phospho-specific antibodies displayed marked species specificity (**D-F**). Although human FFA4 also becomes phosphorylated in response to addition of TUG-891 and we have previously described phospho-specific antibodies able to recognise this protein (ref 26), neither of the mFFA4 phospho-specific antibodies was able to identify the phosphorylated human receptor (**D**, **E**). Immunoblots with anti-GFP/eYFP confirmed that the human receptor was expressed at similar levels (**F**). IP = immunoprecipitation, WB = western blot. Mono = monoclonal, Poly = polyclonal.

Figure 4: Identification of agonist regulation of mFFA4 phosphorylation status using phosphorylation site specific antibodies

Flp-In^{TM} T-REx^{TM} 293 cells were induced to express FLAG-mFFA4-eYFP by addition of doxycycline. Lysates of cells exposed to the indicated concentrations of TUG-891 for 5 min were resolved by SDS-PAGE and phosphorylated receptors detected by immunoblotting with the phospho-Thr^{347}/Ser^{350} antibodies (**A**). Experiments akin to **A** were performed using combinations

Molecular Pharmacology Fast Forward. Published on February 12, 2016 as DOI: 10.1124/mol.115.101949
This article has not been copyedited and formatted. The final version may differ from this version.

of the FFA4 agonist TUG-891 and the FFA4 antagonist compound 39 (Sparks et al., 2014) Samples were subsequently immunoblotted with the phospho-Thr^{347}/Ser^{350} (**left hand side**) or the phospho-Ser^{350} antibodies (**right hand side**) (**B**). Cells as in **A** were exposed to the indicated concentrations of the fatty acid ligands DHA or αLA or the synthetic agonist TUG-891. Phosphorylated receptor was detected using phospho-Thr^{347}/Ser^{350} antibodies (**C**). Structure of compound 39 is shown (**D**).

Figure 5: Phosphorylated mFFA4 is identified in immunocytochemical studies

Flp-In™ CHO cells transfected to express FLAG-mFFA4-eYFP (**A-C**) or parental cells (**D**) were grown on coverslips. Those expressing FLAG-mFFA4-eYFP were treated with TUG-891 (10 μM, 10 min) (**A**), vehicle (**B**) or compound 39 (10 μM, 60 min) (**C**). After fixation cells were treated with the phospho-Thr^{347}/Ser^{350} antibodies and with DAPI to identify cell nuclei. Blue = DAPI, Green = eYFP, Red = phospho-Thr^{347}/Ser^{350} antibodies. The merged images (right hand panels) illustrate co-localization of eYFP-tagged receptor and the phospho-site specific antibodies (**A, B**). Note the enhanced staining with the phospho-receptor specific antibodies after treatment with TUG-891 (**A** versus **B**) and the reduction in basal antibody staining after treatment with compound 39 (**C** versus **B**).

Figure 6: Mutagenesis studies define two clusters of amino acids that become phosphorylated in response to TUG-891

The C-terminal sequence of mFFA4 is shown using the amino acid one letter code. Aliphatic hydroxy amino acids (serine and threonine) in this region that are potential targets for modification by phosphorylation are in bold. Designation of variants in which clusters of these

Molecular Pharmacology Fast Forward. Published on February 12, 2016 as DOI: 10.1124/mol.115.101949
This article has not been copyedited and formatted. The final version may differ from this version.

residues were mutated to alanine is shown, and in the sequence these changes are noted (**A**). Wild type FLAG-mFFA4-eYFP and each of the indicated mutants were expressed stably in Flp-In^{TM} CHO cells. [^{32}P]-orthophosphate labelling and incorporation of this into the forms of the receptor (**B**) with or without treatment with TUG-891 for 5 min was performed as in Figure 1. Parallel immunoblotting studies using anti-GFP/eYFP indicated that each form of the receptor was expressed to similar levels (**C**). Quantification of the extent of incorporation of [^{32}P] into the receptor was performed as in Figure 1 (**D**). Different from wild type; * $p < 0.05$. **E, F**. Cells expressing mFFA4-eYFP, mFFA4-TDTS-AAA, mFFA4-ADAA-SSS, or mFFA4-ADAA-AAA were treated for 5 min with TUG-891 and immunoblots performed on cells lysates using the phospho-Thr^{347}/Ser^{350} (**E**) or anti-FLAG (**F**) antisera. WB = western blot, Poly = polyclonal.

Figure 7: Elimination of C-terminal hydroxyl amino acids from mFFA4 compromise agonist-induced interaction with arrestin 3

BRET studies were performed in HEK293T cells transfected to co-express arrestin 3-*Renilla* luciferase and each of wild type FLAG-mFFA-eYFP , mFFA4-ADAA-SSS, mFFA4-TDTS-AAA or mFFA4-ADAA-AAA. Following addition of the indicated concentrations of TUG-891 for 5 minutes, interaction was recorded (**A**). Although the alterations to the receptor sequence did not affect the potency of TUG-891 each of the three variants produced a smaller effect than wild type. Differences between the individual mutants in terms of maximal signal were also significant as noted, *** $p < 0.001$. Similar studies were performed, but following addition of TUG-891 (10 μM) interactions were followed over time (**B**). Representative traces are shown.

Molecular Pharmacology Fast Forward. Published on February 12, 2016 as DOI: 10.1124/mol.115.101949
This article has not been copyedited and formatted. The final version may differ from this version.

Figure 8: Elimination of C-terminal hydroxyl amino acids from mFFA4 compromises agonist-induced internalization of the receptor

N-terminally FLAG and C-terminally e-YFP-tagged forms of wild type mFFA, mFFA4-TDTS-AAA, mFFA4-ADAA-SSS, or mFFA4-ADAA-AAA were expressed stably in Flp-In™ T-REx™ 293 cells. Following doxycycline induced expression of the receptor constructs for 24 hours cells were challenged with vehicle (0 min) or 10 μM TUG-891 (60 min). **A**. Cells were imaged to identify the location of eYFP. Representative images of groups of cells are shown. **B.** Cell surface ELISA assays were performed using an anti-FLAG antibody to detect cell surface receptor on non-permeabilized cells treated as in **A** with vehicle (0 min) or 10 μM TUG-891 (60 min). Data are means +/- SEM of triplicate data points from a single experiment, representative of four. Internalization of mFFA4-ADAA-SSS in response to the agonist was unaffected compared to wild type mFFA4, whilst internalization of both mFFA4-TDTS-AAA and mFFA4-ADAA-AAA was substantially reduced. *** $p < 0.001$.

Figure 9: Signalling of mFFA4 to pAkt Ser^{473} is G protein-independent

Flp-In™ CHO cells expressing FLAG-mFFA4-eYFP were used to assess the potential contribution of G_q/G_{11} (**A-C**) or G_i-family G proteins (**D-E**) to TUG-891-mediated regulation of pERK1/2 (**A**) or pAkt Ser^{473} (**B-E**) phosphorylation in either HTRF (**A, B, D**) or immunoblotting (**C, E**) studies. In certain studies cells were pre-treated with the G_q/G_{11}- inhibitor YM-254890 (**A-C**) or the G_i-inhibitor pertussis toxin (PTX) (**D-E**). Effects of TUG-891 +/- inhibitors were assessed. Although YM-254890 fully blocked the effect of TUG-891 in pERK1/2 assays (**A**), it had no effect on pAkt Ser^{473} (**B, C**) whilst pertussis toxin also did not modify TUG-891 regulation of this signal end point (**D, E**). *** $p < 0.001$, ns = not significantly different.

Molecular Pharmacology Fast Forward. Published on February 12, 2016 as DOI: 10.1124/mol.115.101949
This article has not been copyedited and formatted. The final version may differ from this version.

Figure 10: Signalling of mFFA4 to pAkt Ser^{473} is dependent upon the capacity for and location of phosphorylation within the receptor

pAkt Ser^{473} (**A, B**) or pERK1/2 (**C, D**) was assessed in HTRF assays in Flp-In^{TM} CHO cells expressing mFFA4-eYFP (circles), mFFA4-TDTS-AAA-eYFP (triangles), FLAG mFFA4-ADAA-SSS-eYFP (squares), or FLAG mFFA4-ADAA-AAA-eYFP (inverted triangles). Effects of TUG-891 (10 μM) for varying times (**A, C**) or of varying concentrations of the agonist for 5 minutes (**B, D**) were assessed.

Molecular Pharmacology Fast Forward. Published on February 12, 2016 as DOI: 10.1124/mol.115.101949
This article has not been copyedited and formatted. The final version may differ from this version.

Table 1:

Concentration response and kinetic profiles of TUG-891 at the mFFA4-WT and mutant receptors in an arrestin-3 BRET assay. Data represent the mean ± S.E.M. of at least five independent experiments.

	pEC_{50}	E_{max}	n	Plateau	$t_{1/2}$	n
mFFA4-WT	7.0 +/- 0.05	100	28	396.5 +/- 29.2	41.8 +/- 1.4	6
mFFA4-ADAASSS	6.9 +/- 0.04	54.3 +/- 2	13	191.2 +/- 17.2	28.4 +/- 1.7	6
mFFA4-TDTSAAA	6.8 +/- 0.1	31.7 +/- 2	9	87.4 +/- 8.3	47.9 +/- 1.9	7
mFFA4-ADAAAAA	6.8 +/- 0.1	19.7 +/- 1	10	87.39 +/- 11	25.9 +/- 5.1	5

Molecular Pharmacology Fast Forward. Published on February 12, 2016 as DOI: 10.1124/mol.115.101949
This article has not been copyedited and formatted. The final version may differ from this version.

Table 2:

Potency (pEC_{50}), and relative efficacy (E_{max}) of TUG-891 at the mFFA4-WT and mutant receptors in pERK1/2 and pAkt (Ser473) assays. Values represent the mean ± S.E.M. from three independent experiments performed in triplicate.

	pERK 1/2			pAkt (Ser473)		
	pEC_{50}	Emax	n	pEC_{50}	Emax	n
mFFA4-WT	7.8 +/- 0.2	100	3	8.0 +/- 0.2	100	3
mFFA4-ADAASSS	8.1 +/- 0.1	106 +/- 2	3	8.4 +/- 0.1	76 +/- 1	3
mFFA4-TDTSAAA	8.0 +/- 0.2	111 +/- 1	3	8.0 +/- 0.1	99 +/- 1	3
mFFA4-ADAAAAA	8.2 +/- 0.2	116 +/- 2	3	8.4 +/- 0.4	63 +/- 2	3

Figure 1

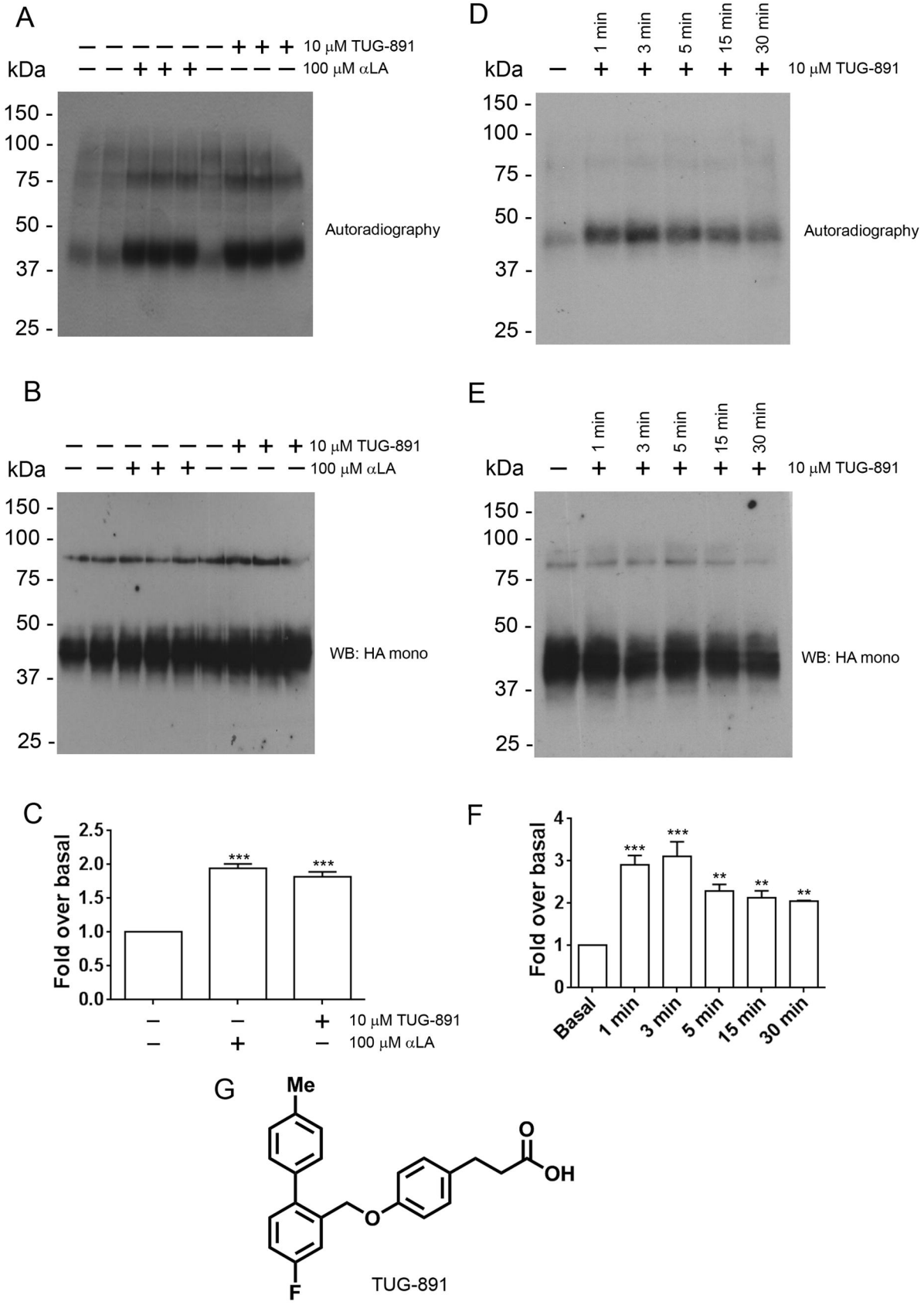
A
10 μM TUG-891
kDa
100 μM αLA
150
100
75
50
37
25
Autoradiography
B
WB: HA mono
C
Fold over basal
2.5
2.0
1.5
1.0
0.5
0.0
***
10 μM TUG-891
100 μM αLA
D
1 min
3 min
5 min
15 min
30 min
E
F
**
Basal
G
Me
O
OH
F
TUG-891

Figure 2

A

GAIFTDT**pS**VRR (pSer-350)

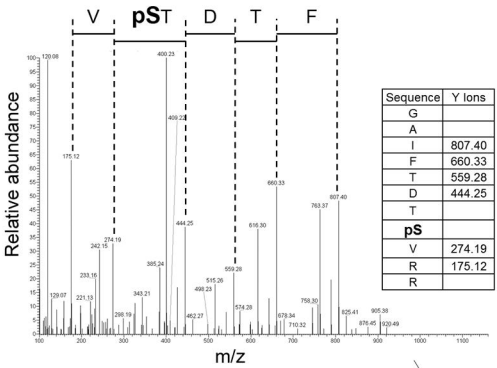

Sequence	Y Ions
G	
A	
I	807.40
F	660.33
T	559.28
D	444.25
T	
pS	
V	274.19
R	175.12
R	

B

GAIFTD**pT**SVRR (pThr-349)

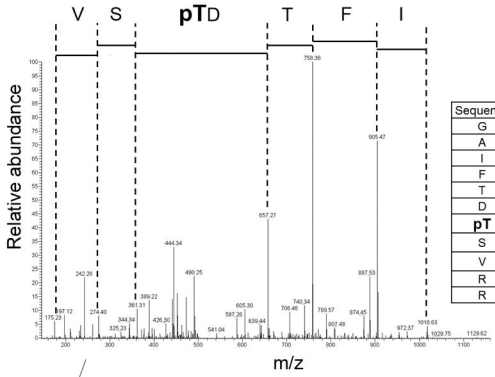

Sequence	Y Ions
G	
A	
I	1018.46
F	905.38
T	758.31
D	657.26
pT	
S	361.22
V	274.19
R	175.12
R	

F

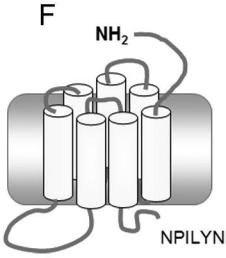

mFFA4 C-Tail

NPILYNMSLFRNEWRKIFCCFFFPEKGAIF**T**D**TS**VRRNDL**S**VIS**S**

G

Sequence	Residue number	Mascot score	Delta PPM	Number of times observed
GAIFTDT**pS**VRR	343-353	44.8	0.8	4
GAIF**pT**DT**pS**VRR	343-353	25.0	-0.19	2
RNDL**pS**VISSGYPYDVPDYA	352-361	38.8	2.0	12
GAIFTD**pT**SVRR	343-353	44.4	1.3	2
GAIFTD**pTpS**VRR	343-353	19.4	0.2	2
RNDLSVIS**pS**GYPYDVPDYA	352-361	36.9	1.9	6

C

GAIF**pT**DT**pS**VRR (pThr-347 and pSer-350)

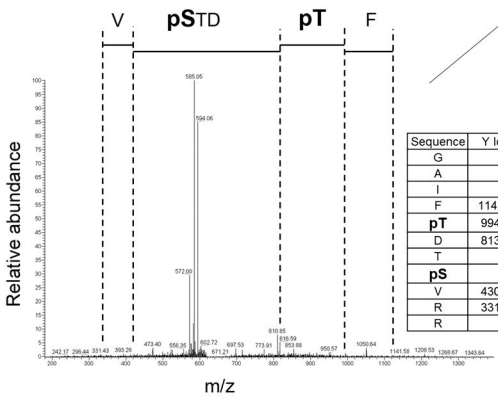

Sequence	Y Ions
G	
A	
I	
F	1141.40
pT	994.40
D	813.40
T	
pS	
V	430.30
R	331.20
R	

D

RNDL**pS**VISSYPYDVPDYA (pSer-357)

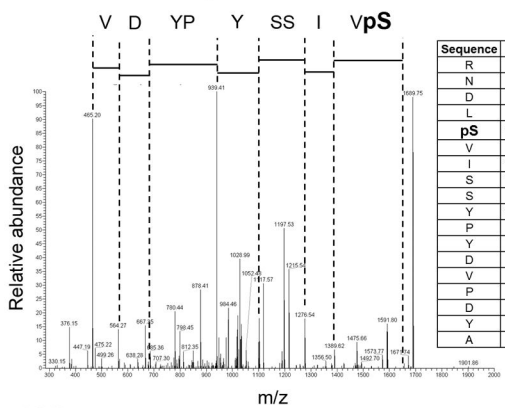

Sequence	Y Ions
R	
N	
D	
L	
pS	1,655.69
V	
I	1,389.62
S	1,276.54
S	
Y	1,102.47
P	939.41
Y	
D	679.29
V	564.27
P	465.20
D	
Y	
A	

E

RNDLSVIS**pS**YPYDVPDYA (pSer-361)

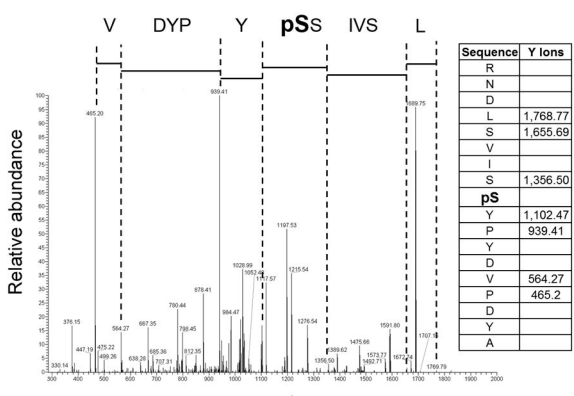

Sequence	Y Ions
R	
N	
D	
L	1,768.77
S	1,655.69
V	
I	
S	1,356.50
pS	
Y	1,102.47
P	939.41
Y	
D	
V	564.27
P	465.2
D	
Y	
A	

Figure 3

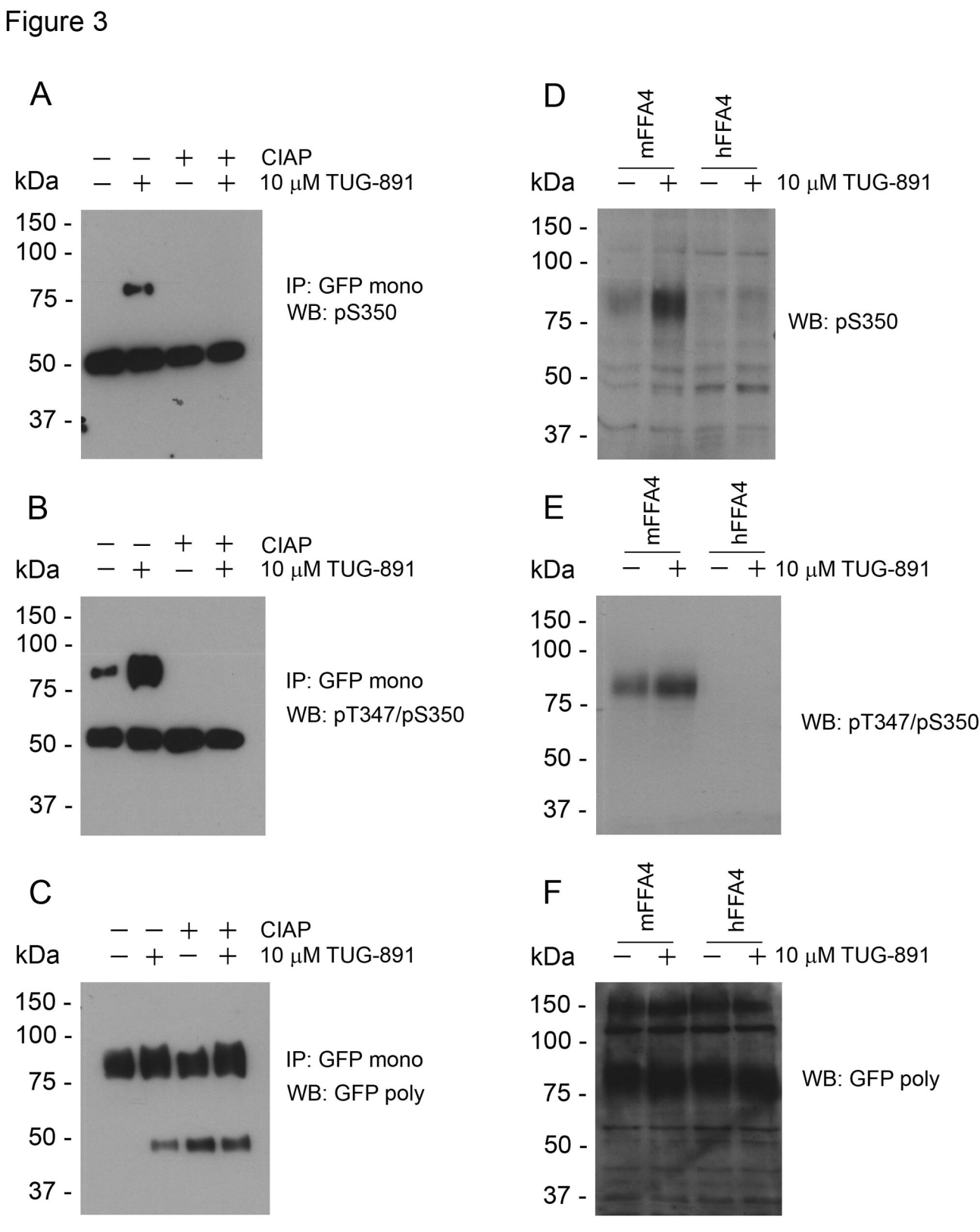
A
CIAP
kDa
10 μM TUG-891
150 -
100 -
75 -
50 -
37 -
IP: GFP mono
WB: pS350
B
CIAP
kDa
10 μM TUG-891
150 -
100 -
75 -
50 -
37 -
IP: GFP mono
WB: pT347/pS350
C
CIAP
kDa
10 μM TUG-891
150 -
100 -
75 -
50 -
37 -
IP: GFP mono
WB: GFP poly
D
mFFA4
hFFA4
kDa
10 μM TUG-891
150 -
100 -
75 -
50 -
37 -
WB: pS350
E
mFFA4
hFFA4
kDa
10 μM TUG-891
150 -
100 -
75 -
50 -
37 -
WB: pT347/pS350
F
mFFA4
hFFA4
kDa
10 μM TUG-891
150 -
100 -
75 -
50 -
37 -
WB: GFP poly

Figure 4

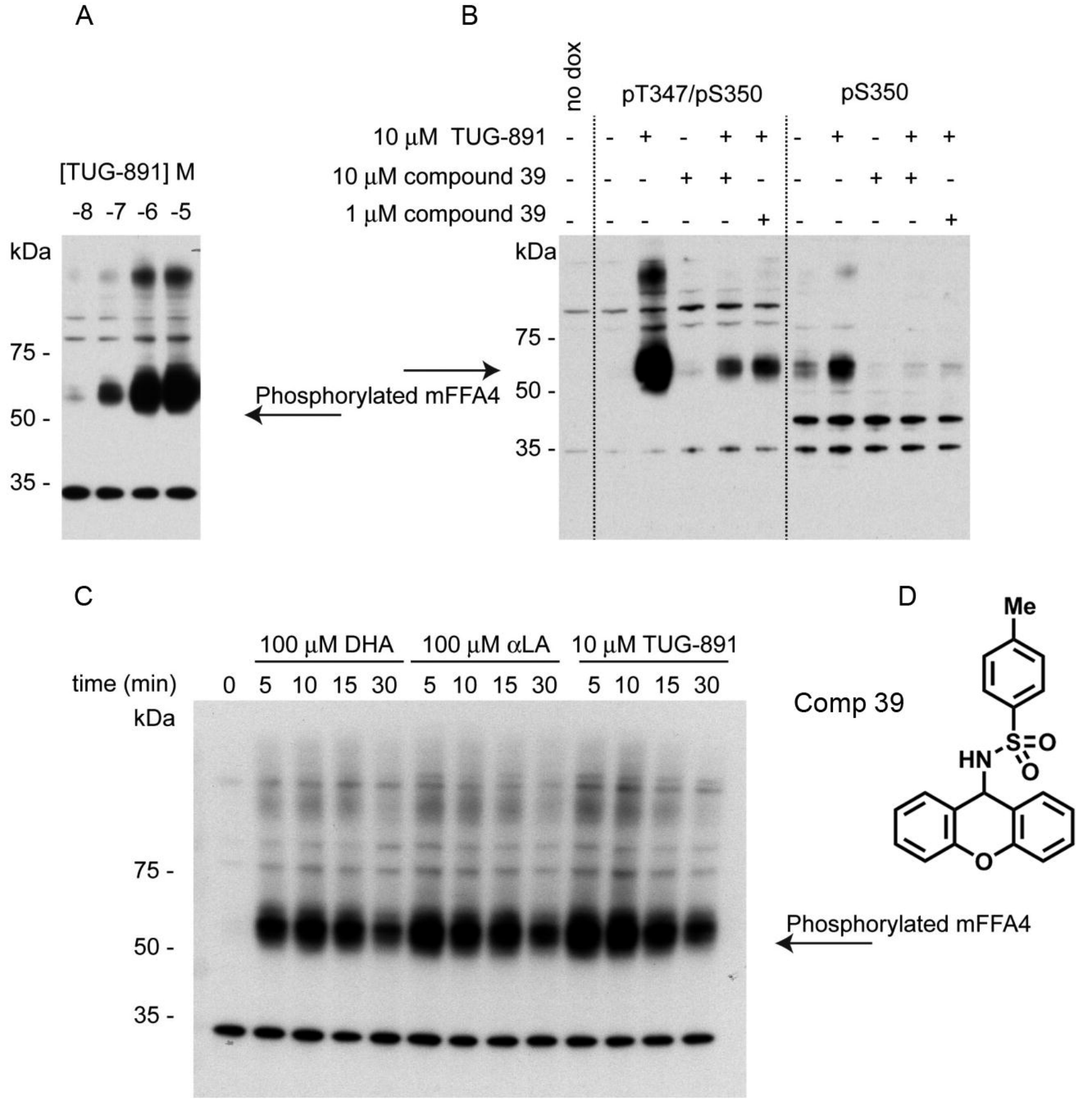
A
[TUG-891] M
-8 -7 -6 -5
kDa
75 -
50 -
35 -
B
no dox
pT347/pS350
pS350
10 μM TUG-891
10 μM compound 39
1 μM compound 39
kDa
75 -
50 -
35 -
Phosphorylated mFFA4
C
100 μM DHA
100 μM αLA
10 μM TUG-891
time (min)
0 5 10 15 30 5 10 15 30 5 10 15 30
kDa
75 -
50 -
35 -
D
Comp 39
Me
HN
S
O
O
O
Phosphorylated mFFA4

Figure 5

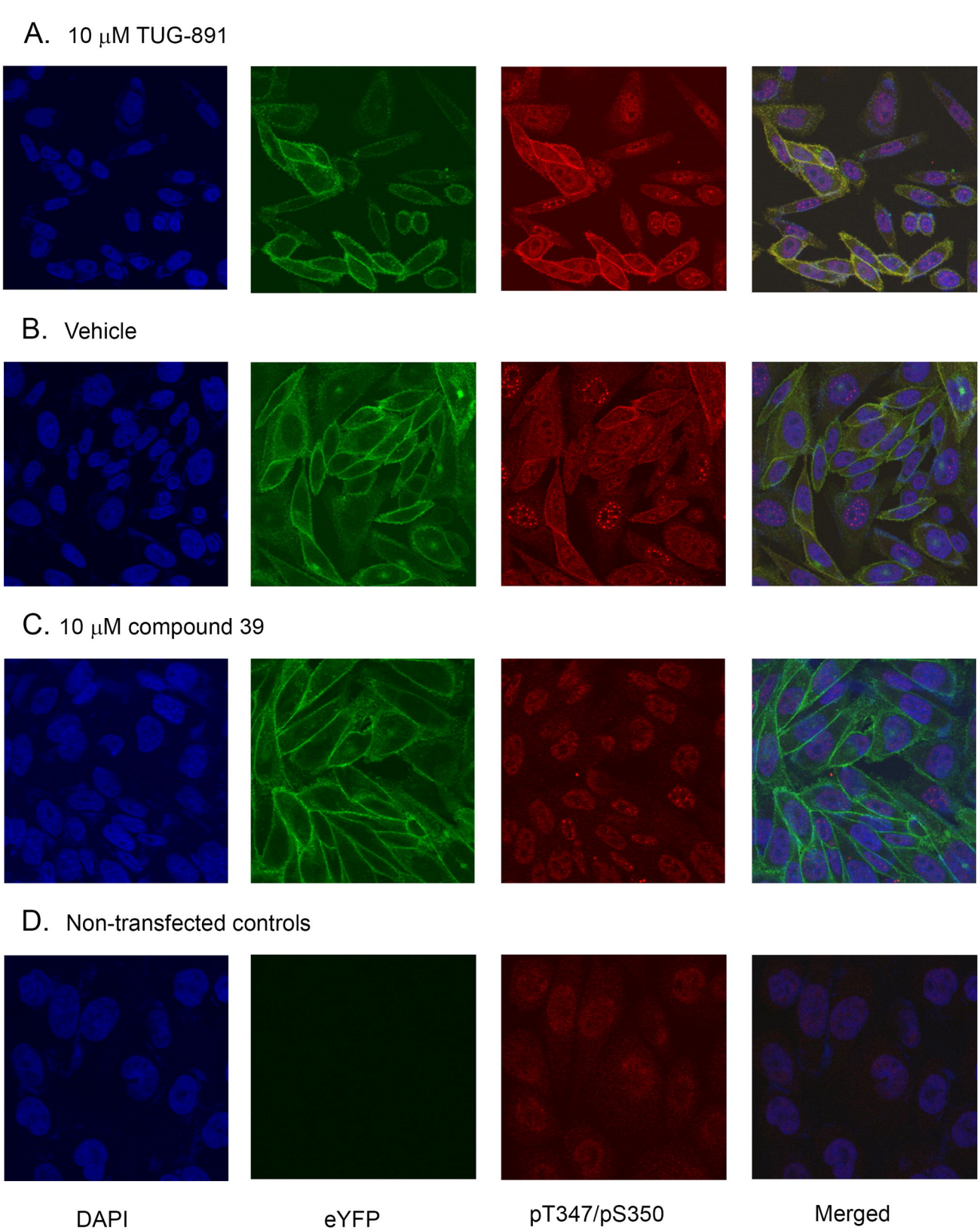
A. 10 μM TUG-891
B. Vehicle
C. 10 μM compound 39
D. Non-transfected controls
DAPI
eYFP
pT347/pS350
Merged

Figure 6

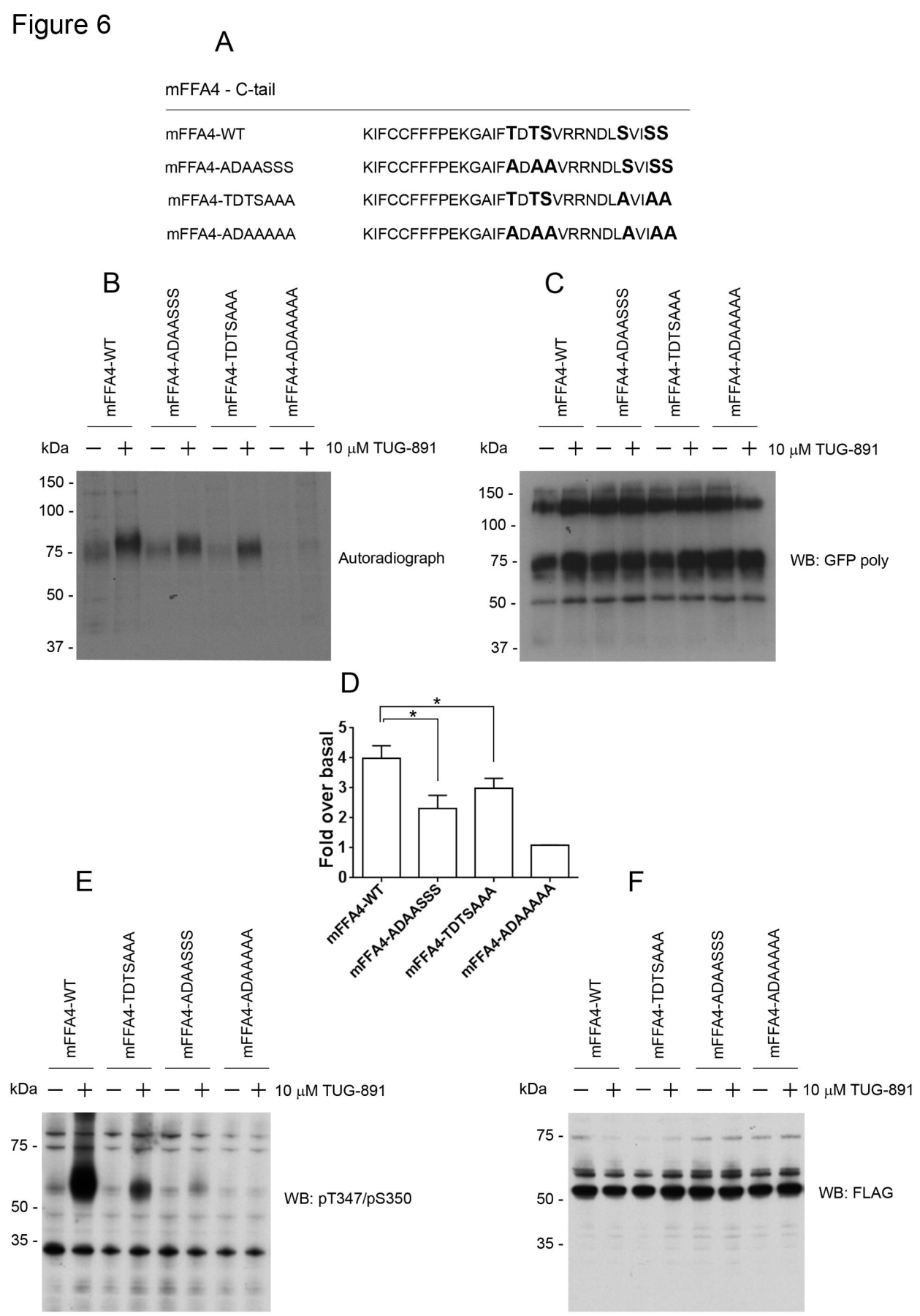
A
mFFA4 - C-tail
mFFA4-WT KIFCCFFFPEKGAIFTDTSVRRNDLSVISS
mFFA4-ADAASSS KIFCCFFFPEKGAIFADAAVRRNDLSVISS
mFFA4-TDTSAAA KIFCCFFFPEKGAIFTDTSVRRNDLAVIAA
mFFA4-ADAAAAA KIFCCFFFPEKGAIFADAAVRRNDLAVIAA
B
mFFA4-WT
mFFA4-ADAASSS
mFFA4-TDTSAAA
mFFA4-ADAAAAA
kDa
10 μM TUG-891
150
100
75
50
37
Autoradiograph
C
WB: GFP poly
D
Fold over basal
0
1
2
3
4
5
*
*
E
WB: pT347/pS350
75
50
35
F
WB: FLAG

Figure 7

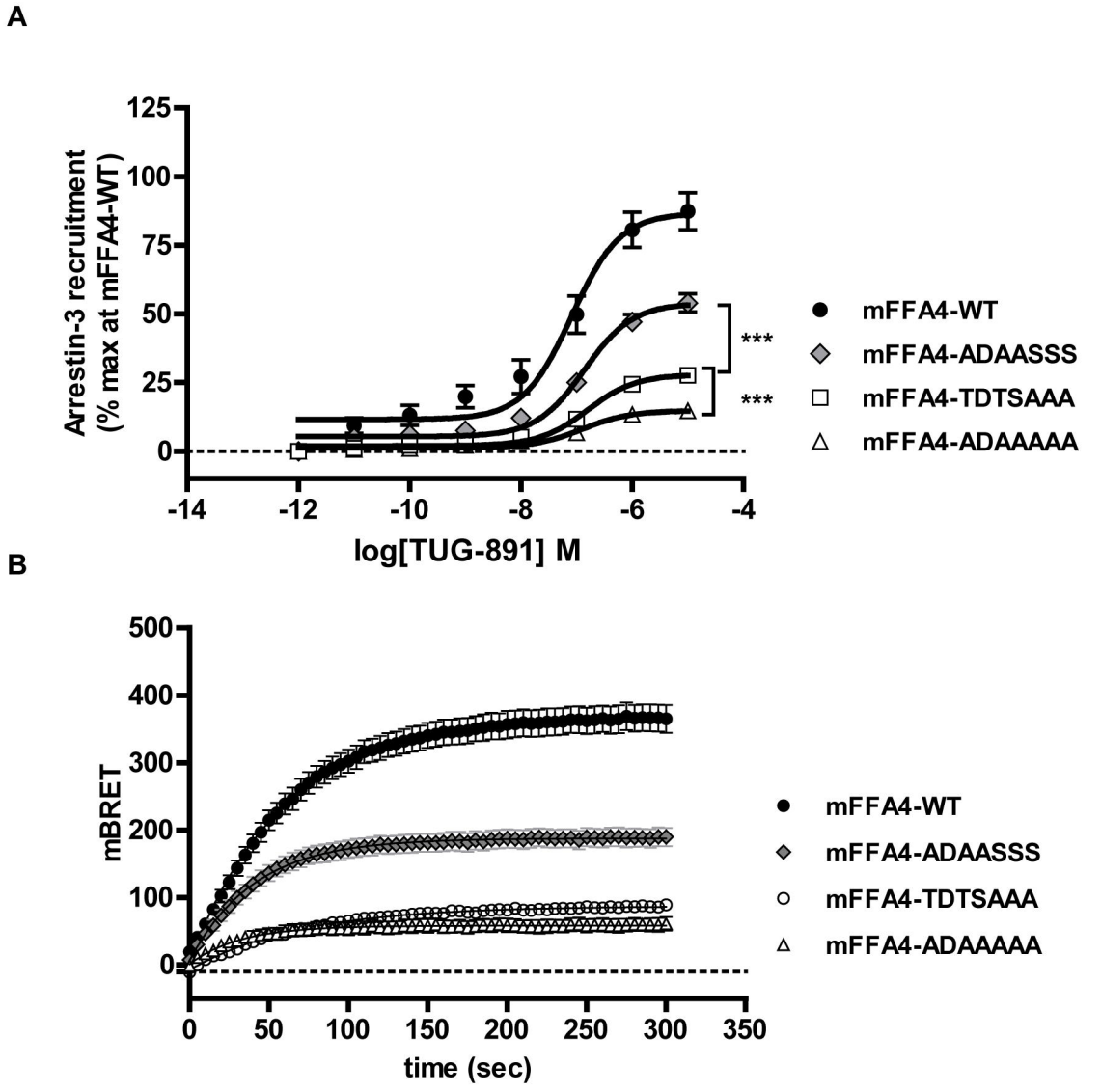
A
Arrestin-3 recruitment
(% max at mFFA4-WT)
125
100
75
50
25
0
-14
-12
-10
-8
-6
-4
log[TUG-891] M
***
***
mFFA4-WT
mFFA4-ADAASSS
mFFA4-TDTSAAA
mFFA4-ADAAAAA
B
mBRET
500
400
300
200
100
0
0
50
100
150
200
250
300
350
time (sec)
mFFA4-WT
mFFA4-ADAASSS
mFFA4-TDTSAAA
mFFA4-ADAAAAA

Figure 8

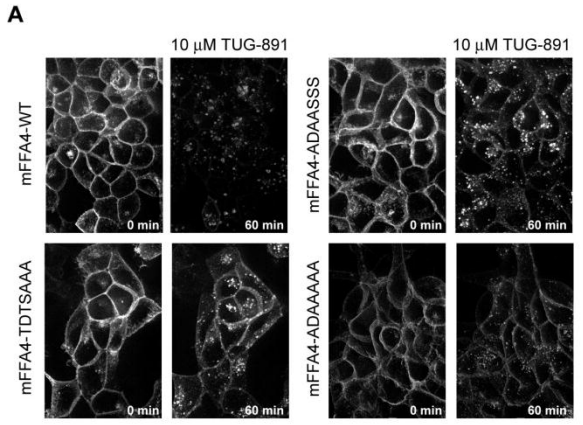
A
10 μM TUG-891
10 μM TUG-891
mFFA4-WT
mFFA4-ADAASSS
mFFA4-TDTSAAA
mFFA4-ADAAAAA
0 min
60 min
0 min
60 min
0 min
60 min
0 min
60 min
B
150
100
50
0
% surface receptor
***
***
***
***
0 60 0 60 0 60 0 60
time (min)
mFFA4-WT
mFFA4-TDTSAAA
mFFA4-ADAASSS
mFFA4-ADAAAAA

Figure 9

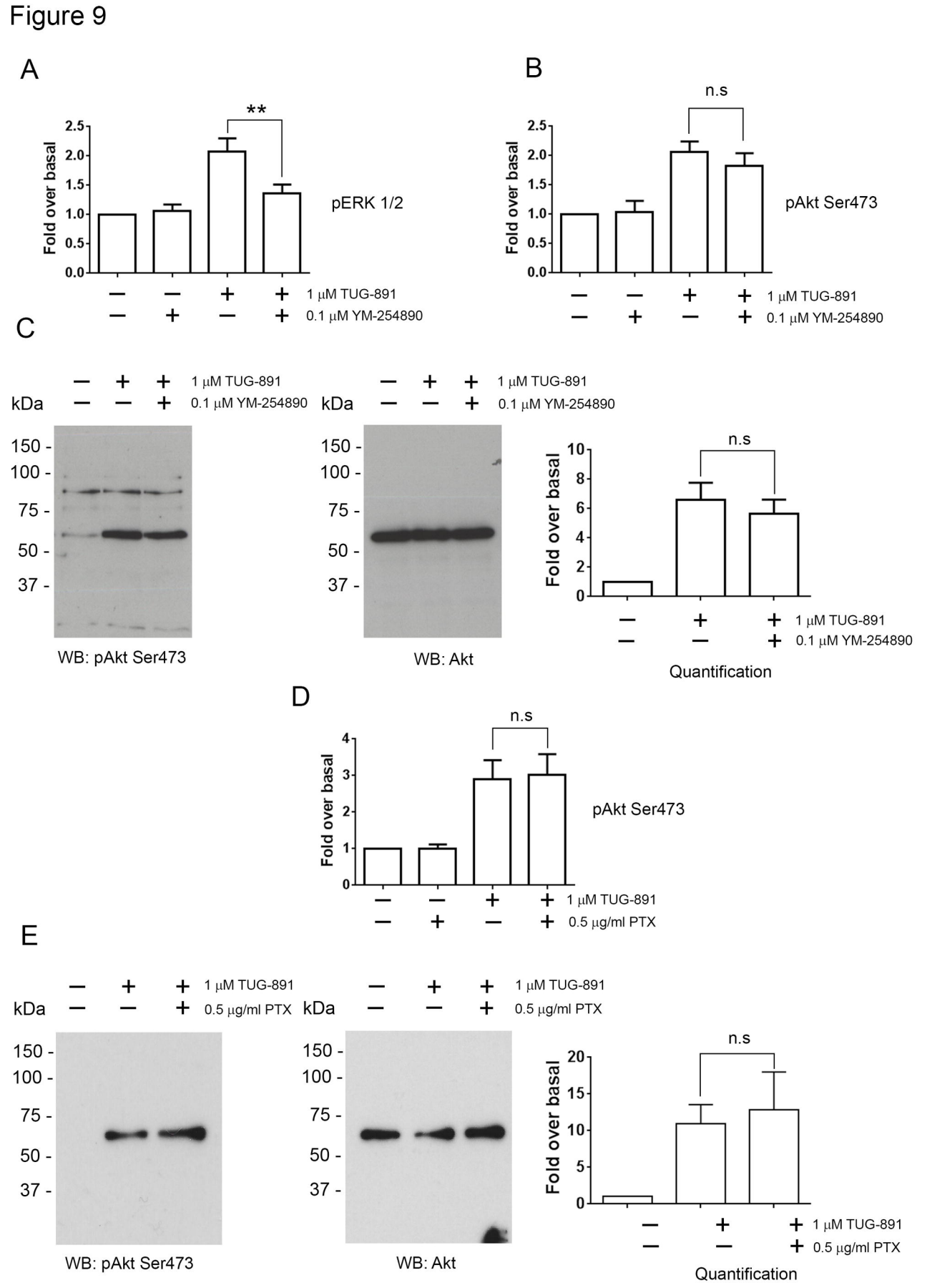
A
**
Fold over basal
2.5
2.0
1.5
1.0
0.5
0.0
pERK 1/2
1 μM TUG-891
0.1 μM YM-254890
B
n.s
pAkt Ser473
C
kDa
150 -
100 -
75 -
50 -
37 -
WB: pAkt Ser473
WB: Akt
Quantification
D
pAkt Ser473
0.5 μg/ml PTX
E

Figure 10

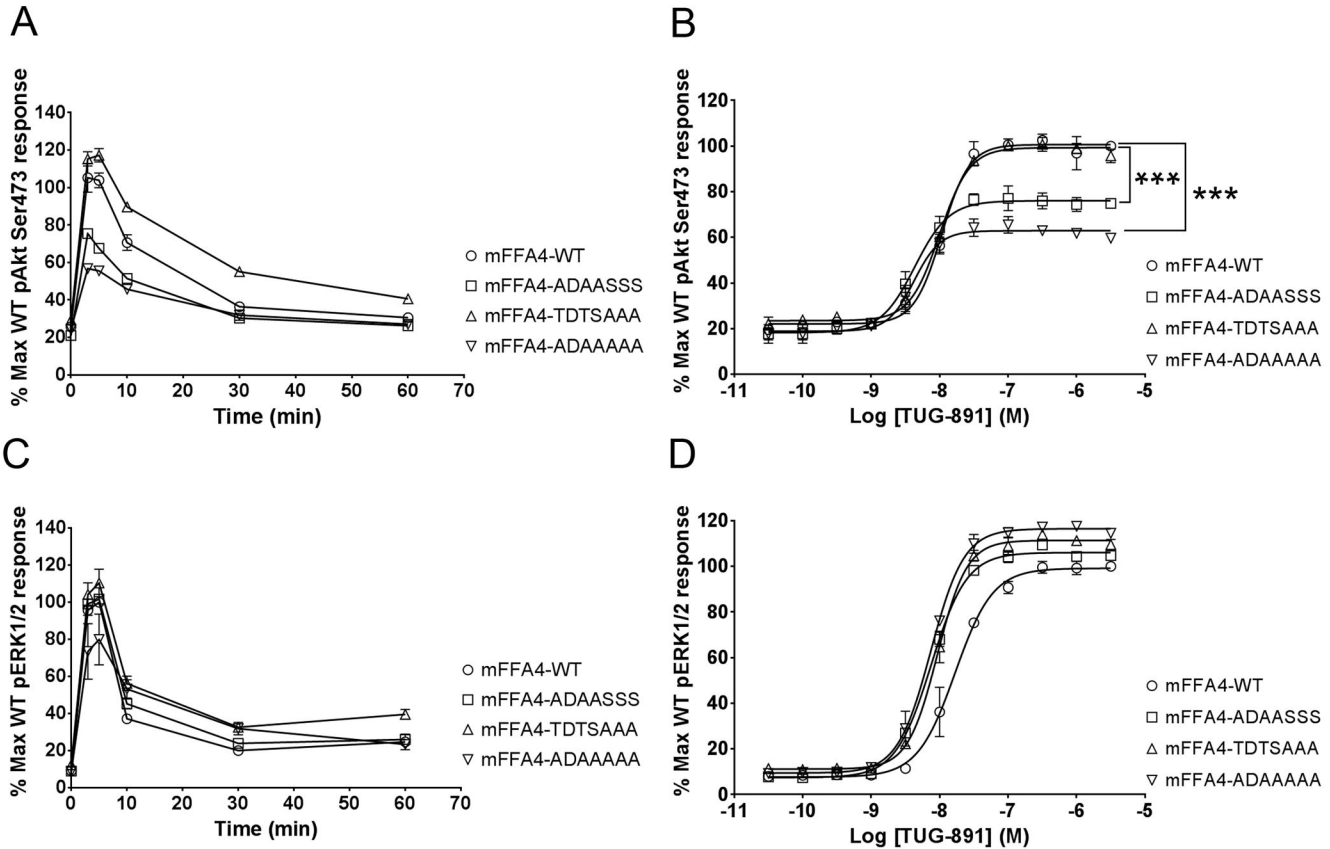
A
% Max WT pAkt Ser473 response
Time (min)
mFFA4-WT
mFFA4-ADAASSS
mFFA4-TDTSAAA
mFFA4-ADAAAAA
B
% Max WT pAkt Ser473 response
Log [TUG-891] (M)
***
***
C
% Max WT pERK1/2 response
Time (min)
D
% Max WT pERK1/2 response
Log [TUG-891] (M)